TRANSPORT AND PHASE EQUILIBRIA PROPERTIES FOR STEAM FLOODING OF HEAVY OILS

FINAL PROGRESS REPORT

PERIOD: OCT 1998-SET 2002

CONTRACT NUMBER: DE-PS26-98FT40147

PROJECT START DATE:	**October 1998**
PROJECT DURATION:	**October 1998 - September 2002**
TOTAL FUNDING REQUESTED:	**$ 199,518**

TECHNICAL POINTS OF CONTACT:

Jorge Gabitto

Prairie View A&M State University

Department of Chemical Engineering

Prairie View, TX 77429

TELE:(936) 857-2427

FAX: (936) 857-4540

EMAIL: jgabitto@aol.com

Maria Barrufet

Texas A&M University

Petroleum Engineering Department

College Station TX, 77204

TELE:(979) 845-0314

FAX:(979) 845-0325

EMAIL: barrufet@spindletop.tamu.edu

TRANSPORT AND PHASE EQUILIBRIA PROPERTIES FOR STEAM FLOODING OF HEAVY OILS

DISCLAIMER

TRANSPORT AND PHASE EQUILIBRIA PROPERTIES FOR STEAM FLOODING OF HEAVY OILS

ABSTRACT

Hydrocarbon/water and CO_2 systems are frequently found in petroleum recovery processes, petroleum refining, and gasification of coals, lignites and tar sands. Techniques to estimate the phase volume and phase composition are indispensable to design and improve oil recovery processes such as steam, hot water, or CO_2/steam combinations of flooding techniques typically used for heavy oils.

An interdisciplinary research program to quantify transport, PVT, and equilibrium properties of selected oil/ CO_2/water mixtures at pressures up to 10,000 psia and at temperatures up to 500 ^oF has been put in place.

The objectives of this research include experimental determination and rigorous modeling and computation of phase equilibrium diagrams, and volumetric properties of hydrocarbon/CO_2/water mixtures at pressures and temperatures typical of steam injection processes for thermal recovery of heavy oils.

Highlighting the importance of phase behavior, researchers ([1], and [2]) insist on obtaining truly representative reservoir fluids samples for experimental analysis. The prevailing sampling techniques used for compositional analysis of the fluids have potential for a large source of error. These techniques bring the sample to atmospheric conditions and collect the liquid and vapor portion of the samples for further analysis. We developed a new experimental technique to determine phase volumes, compositions and equilibrium K-values at reservoir conditions. The new methodology is able to measure phase volume and composition at reservoir like temperatures and pressures. We use a mercury free PVT system in conjunction with a Hewlett Packard gas chromatograph capable of measuring compositions on line at high pressures and temperatures. This is made possible by an essentially negligible disturbance of the temperature and pressure equilibrium during phase volume and composition measurements. In addition, not many samples are withdrawn for compositional analysis because a negligible volume (0.1 μl to 0.5 μl) is sent directly to the gas chromatograph through sampling valves. These amounts are less than 1×10^{-5} % of total volume and do not affect the overall composition or equilibrium of the system.

A new method to compute multi-component phase equilibrium diagrams based on an improved version of the Peng-Robinson equation has been developed [3]. This new version of the Peng-Robinson equation uses a new volume translation scheme and new mixing rules to improve the accuracy of the calculations. Calculations involving multi-component mixtures of CO_2/water and hydrocarbons have been completed. A scheme to lump multi-component materials such as, oils into a small set of "pseudo-components" according to the technique outlined by Whitson [4] has been implemented. This final report presents the results of our experimental and predicted phase behavior diagrams and calculations for mixtures of CO_2/water and real oils at high pressures and temperatures.

TRANSPORT AND PHASE EQUILIBRIA PROPERTIES FOR STEAM FLOODING OF HEAVY OILS

TABLE OF CONTENTS

TRANSPORT AND PHASE EQUILIBRIA PROPERTIES FOR STEAM FLOODING OF HEAVY OILS

STATEMENT OF WORK (SOW)

Under this Statement of Work (SOW), Dr. Jorge Gabitto from the Chemical Engineering Department at Prairie View A&M University (PVAMU), Dr. Maria Barrufet from the Petroleum Engineering Department at Texas A&M University (TAMU) and Dr. Rebecca Bryant from Bio-Engineering Inc. (B-E) conducted research and training in the area of transport and thermodynamic properties determination for heavy oils. A research project was proposed to develop theoretical models, develop computer algorithms, and measure experimentally transport and thermodynamic properties of heavy oils.

Training of graduate and undergraduate students was part of the project. Technology transfer of the results generated by the project was implemented through B-E and publications in referred journals.

Dr. Gabitto has acted as coordinator of the research team. Drs. Barrufet and Bryant were subcontractors to Dr. Gabitto.

TRANSPORT AND PHASE EQUILIBRIA PROPERTIES FOR STEAM FLOODING OF HEAVY OILS

TECHNICAL REPORT

This report is divided in two parts, theoretical and experimental. The theoretical work part has two subparts, development of an improved Peng-Robinson equation of state with volume translation term and development of a procedure to characterize heavy oil mixtures.

EXPERIMENTAL PART

INTRODUCTION.

A good understanding of volumetric and phase behavior of petroleum reservoir fluids is required for accurate prediction of reservoir performance and production forecasting. Phase behavior data dictates reservoir development strategies for ordinary gas drives to more technologically intensive carbon dioxide or steam flooding projects (Wu, [5], Harding et al., [1], among others). Phase behavior data have been obtained traditionally by experimental testing or by use of generalized correlations. Of these two methods the later is often favored by researchers because it is easier to use and less expensive; however, predictions using general correlations can be highly inaccurate mainly due to varying chemical and physical properties of reservoir fluids from one reservoir to another.

Highlighting the importance of phase behavior, researchers insist on obtaining truly representative reservoir fluids samples for experimental analysis. Similar efforts have been done for accurate prediction of phase compositions especially for mixtures of hydrocarbons and water and/or CO_2 (McKetta and Katz, [6]; Mehra et al., [7]; Shibata et al., [8]; Langasan and Smith, [9]). In more recent times (Barrufet and Rahman, [10]) very accurate gas chromatographs along with PVT apparatus have been employed for determination of phase compositions (Barrufet and Rahman, [10]).

The objective of this part of the project is to determine bubble point and pressure-volume relationships for several oil samples already available. Experimental work was done using a Paradis crude oil (Stock Tank Oil) available at the Petroleum Engineering Department at TAMU. During the project Bio-Engineering Inc. provided several heavy oil samples (API^{o} 20-25). The samples were provided under the generic name 'Kansas Oil.' TBP analyses were obtained for two of the samples. The compositional results are listed in the Appendix together with compositional data collected from literature sources. The bubble point results are presented in the experimental results section.

APPARATUS AND EXPERIMENTAL SET-UP

The laboratory set-up consists of three main parts:

I - VACUUM SYSTEM

II- HYDRAULIC SYSTEM

III. RECOMBINATION APPARATUS

I –Vacuum System. The vacuum system consists of a vacuum pump, two traps to protect the vacuum pump from liquid, and tubing.

II- Hydraulic System. Hydraulic System consists of a Ruska positive displacement pump, a pressure gauge, high-pressure valves and tubing. The purpose of this system is to charge the volume in the upper portion of the recombination cell.

The capacity of the pump is 500 cc (0.01765 cu. ft.).

The maximum working pressure is 340.25 ATM (5000 psia).

The displacement pump is equipped with a discharge volume scale. This is used to monitor the volume of the discharge and, indirectly, the volume of the recombination cell. This scale can be read within 0.02 cc (7.062 e -7 cu. ft.).

III- Recombination Apparatus.

a). The Temperature Controlled Air-Bath Oven with maximum operating temperature 200 C (392 F). The temperature can be set with an accuracy of 0.2 C. Uniform air bath temperature distribution +- 1 C.

b). The Recombination Cell

JEFFREY Recombination cell model No 1OOO-10-P-REC

Floating piston.

Capacity of the Cell 1,000 cc (0.0353 Cu. ft.).

Maximum working pressure 689.48 bar (10,000 psia).

Maximum working temperature 200 C (392 F).

c). The Rocking Mechanism

Laboratory set-up.

This rocking mechanism is provided to mix efficiently a multi component fluid such the desired equilibrium condition can rapidly be obtained.

The laboratory set-up was constructed according the standard set-up suggested in the manual book of the recombination apparatus. The recombination Cell is connected from the bottom with hydraulic system and with the Sample Cylinder from the top. The hydraulic system is connected with the bottom of both recombination cell and simple cylinder. The sample cylinder is connected with hydraulic system from the bottom and with the recombination cell from the top. The vacuum system is used with all the system depending of step of experiment.

Procedure to charge the hydraulic oil into the system:

1- Before charging oil into the hydraulic system, all air has to be removed from the system by using vacuum (from the hydraulic pump until the bottom of recombination Cell).

2- Injecting the hydraulic oil into the bottom of the recombination cell until the floating piston arrive on the top of the Recombination Cell.

3- Do the same procedure for the preparation of Sample Cylinder.

4- Charge the crude Oil into the Sample Cylinder.

5- Before Charging the Oil from the Sample Cylinder, all air has to be removed from the system between the top of the Recombination Cell until the connection with the Sample Cylinder.

6- Charge the oil from the Sample Cylinder into the top of the Recombination Cell by using the hydraulic pump.

7- Close the top of the Recombination Cell.

8- Heat the System until the wanted Temperature.

Composition of the Oil Samples:

The characteristics of the oils used in the bubble point pressure experiments are:

Oil A

Paradis crude oil (Stock Tank Oil). The volume injected into the recombination cell of this oil is:

V= 500 cc at T=22 C and 1 ATM, API # 40, density = 0.82 g/cc, so the mass of this oil is 410 g.

Oil B

A mixture of 95.7% mass of Oil A and 4.3% mass of Methane.

The mixture is 1.71% volume of black oil and 98.29 % volume of Methane and at T=22 C and Atmospheric Pressure.

Oil C

Oil B plus 5 cc (5g) of distilled water. Then the total mass of mixture is 433.45 g, 410 g black oil + 18.45 g Methane + 5 g water). The water was added to the recombination cell at a pressure above the pressure inside the cell (2100 psi we used this pressure to keep the system under the liquid phase), and to avoid the back flash.

Oil D

Oil C plus 20 cc of distilled water. Thus then the total mass of mixture is 453.45 g (410 g black oil + 18.45 g Methane + 25 g water). The same procedure of Oil C is used.

Oil E

Kansas heavy oil. See Appendix for compositional data.

V= 500 cc at T=22 C and 1 ATM, API # 20, density = 0.933 g/cc, so the mass of this oil is 466.5 g.

Oil F

Kansas heavy oil. See Appendix for compositional data.

V= 500 cc at T=22 C and 1 ATM, API # 22, density = 0.921 g/cc, so the mass of this oil is 460.5 g.

THEORETICAL WORK

PHASE EQUILIBRIUM CALCULATIONS

Introduction

Water and CO_2 are used extensively in enhanced oil recovery processes such as steam flooding and CO_2 flooding. These methods are the most important thermal/miscible oil recovery processes (Wu, 1977 [5]; Harding et al.; 1983 [1]; Turek et al., 1984 [2], Boberg, 1988 [5]). Steam and/or CO_2 are injected into reservoirs where hydrocarbons and brines coexist. Intermolecular interactions of CO_2 with water and hydrocarbons will affect the species partitioning into the coexisting equilibrium phases, i.e., the hydrocarbon K-values (K_i's) will likely be different from those obtained at the same pressure and temperature, but in the absence of water or of CO_2.

In steam-thermal recovery processes, steam is either injected into or generated within a reservoir where the hydrocarbons and water may coexist in three phases, vapor and two liquid phases, hydrocarbon and water. In miscible enhanced oil recovery processes using CO_2 as a displacing medium, the aqueous effects on the hydrocarbon/ CO_2 phase behavior have not been fully investigated. Because of the aqueous phase vapor pressure and the mutual solubility of water and hydrocarbon/ CO_2 in the liquid phases, neglecting

the aqueous effects can induce serious error in the representation of hydrocarbon/ CO_2 phase behavior. Hornbrook et al., 1991 [12], reported the use of CO_2 in steam flooding showing many beneficial effects on oil recovery and economics.

Phase equilibrium diagrams and volumetric properties are important in the design, development and operation of chemical processes and reservoir simulations. In order to estimate these properties, cubic equations of state (EOS) are commonly used. Since the development of van der Waals equation of state [13], more accurate equations of state have been developed which can describe thermodynamic properties and phase equilibria of a wide range of substances with varying degrees of successes (for example, see [7-9, 14]).

Among the simple two-parameter cubic equations of state, the Peng-Robinson equation of state (PR EOS) [15] is commonly used to model phase behavior and volumetric properties of fluid mixtures encountered in natural gas refinery, petrochemical and chemical applications. The Peng-Robinson equation of state for a pure fluid can be written as

$$P = RT / (v - b) - a / (v^2 + ubv + wb^2) \qquad (4).$$

Where, P is the pressure, v is the molar volume, R is the gas constant, b is the excluded-volume parameter, and a, is the attraction energy parameter. For PR EOS, u = 2 and w = −1, and b and a are defined as,

$$b = b_c \text{ and } a = a_c\, \alpha(\omega, T_r) \qquad (5).$$

Where, critical parameters b_C and a_C are given by

$$b_c = 0.07779607\ (RT_c)/P_c \qquad (6)$$

$$a_c = 0.45723553\ (RT_c)^2/P_c \quad . \qquad (7)$$

and $\alpha(\omega,T_r)$ is defined as

$$\alpha(\omega, T_r) = \left[1 + m(\omega)\left(1 - T_r^{\,X}\right)\right]^2 \qquad (8).$$

Where, ω is the Pitzer acentric factor, and T_r is the reduced temperature, $T_r = T/T_C$, with T the absolute temperature and T_c the critical temperature. In the original PR EOS, X = 0.5, and $m(\omega)$ is expressed in terms of a simple polynomial in ω, specific to a particular fluid. In order to calculate volume from PR EOS, Eqn.(1) can be expressed in terms of the compressibility factor Z as

$$Z^3 + (B-1)Z^2 + (A - 3B^2 - 2B)Z + (B^3 + B^2 - AB) = 0 \qquad (9), \text{ with}$$

$$A = aP/R^2T^2 \ , \ B = bP/RT \ \text{ and } \ Z = vP/RT \qquad (10).$$

Note that Eqn.(9) is used to calculate volume and can yield one to three roots depending on the number of phases in the system. For the vapor/liquid phase equilibria in pure fluids, the largest positive root of Z corresponds to the vapor phase, while the smallest positive root of Z corresponds to the liquid phase. The fugacity coefficient ϕ of PR EOS can be given by

$$\ln\phi = (Z-1) - \ln(Z-B) + \frac{A}{2\sqrt{2}B}\ln\frac{Z + (1-\sqrt{2})B}{Z + (1+\sqrt{2})B} \qquad (11)$$

Since the original PR EOS (a) cannot describe saturated vapor pressures of fluids at low temperatures, (b) becomes unreliable for fluids with large acentric factors ($\omega > 0.5$), and (c) cannot describe accurately the saturated volumes of liquid and vapor phases, numerous attempts have been made in the past to modify PR EOS.

Several authors ([16] to [22]) have modified PR EOS by representing m of α-term (Eqn.(5)) as a function of both acentric factor and reduced temperature, $m(\omega,T_r)$, for X = 0.5. In these modifications of PR EOS, the common practice has been to represent saturated vapor pressure data as accurately as possible by manipulating m as a function of ω and T_r for X=0.5. Later, Twu *et al*. [23] presented a different approach for determining the α-term by expressing Eqn.(8) in an exponential form (without considering m) and were able to correlate saturated vapor pressures of a number of hydrocarbon fluids ranging from methane (C_1) to eicosane (C_{20}), here referred to as PRT EOS. Their α–term is a function of temperature only and contains three parameters. Twu *et al*. [23] found that the results obtained from PRT EOS for the saturated vapor pressures were more accurate than those obtained either from PR EOS or PRSV EOS. Since the above modifications of α-term (or m) are based on the experimental data of saturated vapor pressures for some selected systems having $\omega < 1$, these equations of state can be applied reliably only to the limited ranges of the acentric factor, ($\omega < 1$).

Keeping the form of α-term to be the same as given by Eqn.(8), we presented an improved form of PR EOS, called MPR EOS [3]. In MPR EOS $m(\omega)$ no longer depends on the properties of a particular fluid. Following the suggestion of Leibovici, [24], $m(\omega)$ was determined by satisfying the isofugacity condition at $T_r = 0.7$ for X = 0.5 using Eqns.(8) and (4) and was represented in a polynomial form. So long as u and w of Eqn.(4) are temperature independent parameters, the proposed $m(\omega)$ can be applied to

any cubic equation of state and to much larger values of ω (ω < 2). For the well-defined value of m(ω) the X parameter of α-term (Eqn.(8)) did not yield an universal value of X=0.5. Therefore, we represented X in terms of a simple polynomial in reduced temperature containing four parameters, which were obtained by comparing calculated results with experimental data of the saturated vapor pressures of several fluids over a range of temperatures and pressures. In this work also we represent X in terms of a polynomial in T_r. Unlike the previous work, however, now X contains only three parameters.

The purpose of the theoretical work is to develop an improved form of the Peng-Robinson equation of state following Fotouh and Shukla [19] and predict simultaneously the phase behavior and volumetric properties of fluids of industrial interest over a wide range of acentric factor values and the entire temperature range along the saturation line. This is accomplished by (1) defining X as a function of temperature with three parameters only, (2) using our polynomial of m(ω), which can describe fluids with large acentric factors of practical interest (ω ≤ 2 and above) and is independent of temperature and a particular fluid, and (3) incorporating the temperature independent volume translation term of Mathias et al [25] with a simple modification. In this way, we further simplify our earlier modifications of α-term and introduce a new version of the volume translation term, which is more accurate close to the critical point. We also extend calculations to more systems of practical interest.

A brief account of the modified form of PR equation of state (MPR EOS) is presented below.

Modified Peng-Robinson Equation of State (MPR EOS)

The general form of MPR EOS for a pure fluid is given by Eqn. (4) along with Eqns. (5) through (11). The important parameters of MPR EOS are m and X of the α-term (Eqn.(8)). As mentioned above, in this modification m depends on ω only and is given by [17]

$$m(\omega) = \sum_{j=0}^{4} \sum_{k=0}^{4} A_{jk} u_o^j \omega^k \qquad (12).$$

Here $u_o = 2$ for PR EOS. Coefficients A_{jk} of the above polynomial are reported elsewhere [19].

For correlating the saturated vapor pressures accurately, we express X in term of a simple polynomial given by

$$X = B_0 + B_1 T_r + B_2 T_r^2 + B_3 T_r^3, \text{ with } B_o = 0.5 \qquad (13)$$

In this work, the three parameters B_1, B_2 and B_3 are determined by regression of saturated vapor pressures of the pure fluids. For $B_1 = B_2 = B_3 = 0$, PR EOS is recovered.

Following the approach of Mathias et al. [25], the volume correction term is given by

$$v^{corr} = v + S_1 + F_c \left(\frac{S_2}{S_2 + \delta} \right) \qquad (14).$$

Here δ is a dimensionless quantity related to the inverse isothermal compressibility given by

$$\delta = - \frac{v^2}{RT} \left(\frac{\partial P}{\partial v} \right)_T \qquad (15), \text{ and}$$

$$F_c = v_c^{Exp} - \left(v_c + S_1 \right) \qquad (16)$$

We note that F_c is the additional volume correction term to match the critical volume by equation of state determined using experimental data. In the work of Mathias et al. [25], a universal value of S_2, S_2=0.41, was adopted and S_1 was considered as an independent parameter for each fluid. However, our calculations showed that the above set of the S_1 and S_2 parameters was unable to correlate accurately the saturated volumes of all the fluids used in this work. Therefore, we considered both S_1 and S_2 as independent variables. Also, we found that the above temperature independent volume correction was not adequate for some systems and for heavy hydrocarbons at low temperatures. In order to improve the results for volumes at low temperatures, we redefined Eqn. (14) as follows

$$v^{corr} = v + S_1 + F_c \left(\frac{S_2}{S_2 + \delta} \right) + S_3 T_r \qquad (17).$$

Here Eqn. (17) is now temperature dependent and contains a third parameter, S_3.

Based on the combinations of Eqns. (13) and (14) and those of Eqns. (13) and (17), we performed two kind of calculations in this work. The results obtained from the first set of calculations (i.e., results based on Eqns. (13) and (14)) were referred to as MPR EOS. In this case, five parameters (B_1, B_2, B_3, S_1 and S_2) were determined

simultaneously from the regression of the saturated vapor pressures and liquid volumes of each fluid using the following objective function,

$$ADPV\% = \sum_{i=1}^{n_p} ABS(\Delta P\%)_i + \sum_{j=1}^{n_V} ABS(\Delta V^L\%)_j \quad (18), \text{ with}$$

$$\Delta P\% = (P_{\exp} - P_{cal}) / P_{\exp} \text{ x } 100 \quad (19), \text{ and}$$

$$\Delta V^L\% = (V^L_{\exp} - V^L_{cal}) / V^L_{\exp} \text{ x } 100 \quad (20)$$

In the above equations, P_{exp} is the experimental vapor pressure, P_{cal} is the calculated vapor pressure, V^L_{exp} is the experimental liquid volume, V^L_{cal} is the calculated liquid volume, and n_P and n_V are numbers of the vapor pressure and the liquid volume data along the saturation line, respectively. When experimental data for liquid volume were not available, only B_1, B_2 and B_3 were fitted to the saturated vapor pressures using the first term of Eqn. (18).

In order to illustrate the accuracy of MPR EOS in the whole range of the saturation temperature, Figs. 1-4 present results for the saturated vapor pressures of four selected fluids of Table 1, namely, methane, eicosane, carbon dioxide, and water, respectively. These fluids differ significantly in their acentric factor and polarity. Comparisons of calculated results with experimental data show that MPR EOS is in excellent agreement with experiment over the entire range of the saturation temperature. These comparisons show that MPR EOS is very successful in representing the vapor pressures of even associated fluids such as water (Fig. 4) reasonably well. Fig. 5 illustrates the accuracy of MPR EOS in describing the saturated vapor pressures of heavy hydrocarbons. Fig. 5 shows comparisons between MPR EOS and experiment for four heavy hydrocarbon systems, C_{22}, C_{32}, C_{40} and C_{60}, exhibiting the large values of acentric factor ($0.95 < \omega < 2.6$). Even in these cases, the agreement between calculated and experimental results is excellent.

Modified Wong-Sandler Mixing Rule (MWS MR)

In order to use the MPR cubic equation of state in mixture calculations, one requires a mixing rule (MR) for the determination of mixture energy parameter and excluded-volume parameter. Several attempts have been made in the past to correlate phase

equilibria in mixtures using cubic equations of state by optimizing interaction parameters of the simple classical mixing rules, such as van der Waals one-fluid type mixing rules (see for example, Graboski and Daubert, [26], among others). In recent years, a significant progress has been made in developing new mixing rules for the correlation and prediction of mixture properties using equations of state. Important among them are the mixing rules based on excess Gibbs free energy (G^E) models (liquid solution models) (for review, see Sandler et al, [27]).

Alternatives to the classical mixing rules are the mixing rules based on the excess Gibbs free energy models as proposed by Huron and Vidal [28]. In Huron and Vidal mixing rule the mixture energy parameters were evaluated by equating G^E obtained from the equation of state to that determined from an existing liquid solution model at infinite pressure. The excluded-volume parameter, b_m, was determined using $b_m = \sum x_i b_i$, where x_i is the composition and b_i is the excluded-volume parameter of component i. In those mixing rules, interaction parameters of the G^E models were obtained by fitting experimental data for phase equilibria at low pressures. The estimated parameters were then used to predict phase equilibria at higher pressures.

In order to improve the performance of G^E based mixing rules and to remove the theoretical inconsistency in determining mixture energy and volume parameters Wong and Sandler [29] proposed another form of the mixing rule, called WS MR. This mixing rule represents the correct composition dependency of the mixture second virial coefficient and can predict phase equilibria of several nonideal mixtures using the existing low pressure free energy models (Wong et al., [30], Orbey et al., [31], Huang and Sandler, [32], among others). The G^E model parameters used in WS MR were obtained from the existing results for the Helmholtz free energy model at infinite pressure, A_∞^E, or they were optimized using vapor/liquid equilibrium data at low temperatures and pressures. The unknown interaction second virial coefficient parameter (k_{ij}) was determined from the experimental results of vapor/liquid phase equilibria at low pressures and temperatures. The determined parameters were then used to predict phase equilibria at higher temperatures and pressures. Eubank et al. [33] modified the procedure of Wong and Sandler to obtain mixture parameters of the cubic equations of state directly from the experimental data of cross second virial coefficients, considered in

the single-phase vapor mixture at low pressures. The remaining G^E model parameters were taken from the existing methods, such as the group contribution method. For a well-defined G^E model, the method of Eubank et al. [33] was purely predictive because the cross second virial coefficients were obtained from the experimental data or from the existing empirical correlations.

In a later study Fotouh and Shukla [34] proposed a modified version of the Wong-Sandler mixing rule, called MWS MR. They introduced a theoretical combination rule for the determination of unlike energy and excluded-volume parameters such that the need of experimental data for the cross second virial coefficients could be avoided. In most of the binary mixtures at low pressures there was no need of correlating unlike interaction parameter. The unknown function A_{∞}^{E} was determined from the non-random two-liquid (NRTL) free energy model, parameters of which were available from the earlier studies.

For the MPR cubic equation of state containing two mixture parameters a_m and b_m, WS MR is composed of two equations, one for the liquid state and another for the vapor state. In the liquid state, the mixture energy parameter a_m is expressed as (Wong and Sandler. [29]),

$$a_m = b_m\left[\sum_i x_i a_i / b_i - A_{\infty}^{E}(x)/\sigma\right] \qquad (21),$$

where σ is a constant dependent on the equation of state. For MPR EOS, $\sigma = \ln\left(\sqrt{2}-1\right)/\sqrt{2}$. $A_{\infty}^{E} = G^E$ (low pressure) is the excess Helmholtz free energy in the infinite pressure limit for a fixed liquid composition and temperature.

Using statistical mechanics that the composition dependence of the mixture second virial coefficient B_m should be quadratic, i.e.,

$$B_m(T,x) = \sum_i \sum_j x_i x_j B_{ij}(T) = \sum_i \sum_j x_i x_j \left(b_{ij} - a_{ij}/RT\right) \qquad (22),$$

another equation for the gaseous state is obtained as (Wong and Sandler. [29]),

$$b_m - a_m/RT = \sum_i \sum_j x_i x_j \left(b_{ij} - a_{ij}/RT\right) \qquad (23)$$

Substituting eqn. (12) into eqn. (14), the mixture excluded-volume parameter is given by

$$b_m = \sum_i \sum_j x_i x_j \left(b_{ij} - a_{ij}/RT\right) \Big/ \left[1 + A_\infty^E(x)/\sigma RT - \sum_i x_i a_i / b_i RT\right] \qquad (24)$$

Eqns. (21) and (24) form WS MR. For the known value of A_∞^E, Wong and Sandler determined a_m and b_m by evaluating composition-independent cross second virial coefficient of the equation of state from the following relation:

$$b_{ij} - a_{ij}/RT = \left[\left(b_i + b_j\right)/2 - \left(a_i + a_i\right)/2RT\right]\left(1 - k_{ij}\right) \qquad (25),$$

where k_{ij} is an unknown interaction second virial coefficient parameter.

In WS MR, A_∞^E can be obtained from any free energy model. In order to make the model predictive, the activity coefficient model parameters in WS MR were obtained from the literature (DECHEMA Data Series [35]). The interaction parameter k_{ij} was determined by equating calculated and experimental vapor/liquid equilibrium data at a low temperature and pressure (Wong and Sandler, [29]) or by solving the following equation (Orbey et al., [31]) at a specific composition of each binary mixture considered at low temperature and pressure,

$$G^E(EOS) = G^E(\textit{free energy model}) \qquad (26)$$

Recently, Eubank et al. [33] have suggested that the cross second virial coefficient of the equation of state (B_{ij}) could be represented by the corresponding experimental data

$$B_{ij} = b_{ij} - a_{ij}/RT \equiv B_{ij}^{ex} \qquad (28)$$

where B_{ij}^{ex} is the experimental cross second virial coefficient. This procedure avoids the need of k_{ij} parameter so long as the experimental results or correlations for the cross second virial coefficients are available from earlier studies. However, experimental data for the cross second virial coefficient are not available for all the fluid mixtures under all thermodynamic conditions of our interest. Moreover, for the most mixtures they suffer from large experimental uncertainties.

In order to make WS MR to be purely predictive and independent of experimental data of the cross second virial coefficient, here we propose a theoretical combination rule

(CR) for determining the unlike energy a_{ij} and excluded-volume b_{ij} parameters of the equation of state following a combination rule based on intermolecular interactions. It has been shown in the past that Lennard-Jones potential could describe thermodynamic properties of simple fluid mixtures adequately, and it served as a reliable reference mixture in the theory of molecular fluid mixtures (Shukla, [36]). Assuming that energy and size parameters of the unlike components of the fluid mixtures studied here can be represented by the corresponding energy and size parameters of the Lennard-Jones mixtures in an effective way, we express a_{ij} and and b_{ij} as,

$$a_{ij}/RT = \left(2\sqrt{I_i I_j}/\left(I_i + I_j\right)\right)\left(2^6 b_i b_j/\left(b_i^{1/3} + b_j^{1/3}\right)^6\right)\sqrt{a_i a_j/(RT)^2}\left(1 - k_{ij}\right) \quad (19)$$

$$b_{ij} = \left(\left(b_i^{1/3} + b_j^{1/3}\right)/2\right)^3 \quad (29)$$

where I_i is the ionization potential of component i. Since the ionization potential for most of the fluids of our interest are unknown (Gray and Gubbins, [37]), we further assume that $I_i = I_j$. This simplifies the calculation of unlike parameters greatly. Like WS MR, in eqns. (28) and (29) we have also introduced an interaction parameter, k_i which takes into account the effects of any differences in ionization potentials of the components and unlike interactions, and can be treated as an independent parameter. Eqns. (28) and (29) together with eqns. (22) and (25) are referred to as MWS MR.

In our present calculations, the excess free energy at infinite pressure is obtained from the non-random two-liquid (NRTL) model (Renon and Prausnitz, [38]),

$$A_\infty^E/RT = \sum_i \sum_{j,i\neq j} x_i x_j\left[\tau_{ji} G_{ji}/\left(x_i + x_j G_{ji}\right)\right] \quad (30)$$

$$G_{ij} = \exp\left(-\alpha_{ij}\tau_{ij}\right) \quad (31)$$

$$\alpha_{ji} = \alpha_{ij} \quad (32)$$

The NRTL parameters, α_{12}, τ_{12} and τ_{21}, were taken from the DECHEMA Data Series. When NRTL parameters were not available from the previous works, we determined them at the specified low temperature and pressure. Calculations based on eqns. (22, 25, 28-32) are referred to as MPR EOS/MWS MR.

In order to evaluate the accuracy of our approach we considered several mixtures consisting of non-polar, non-associating polar and associating polar fluids. Here, we present results for a few selected systems, namely, carbon dioxide/propane, butane/methanol, benzene/methanol, and ethanol/water. For most of these mixtures, liquid solution model parameters are available from DECHEMA [35] or from the appropriate aforementioned citations. We present comparisons between our model, MPR EOS/MWS MR, and experiment for vapor/liquid phase equilibria of the above systems under subcritical conditions only.

First, we investigate the accuracy of our model by presenting in Table 2 the percentage average absolute deviation (AAD%) between MPR EOS/MWS MR and experimental data for vapor pressure and vapor composition of two selected mixtures, carbon dioxide/propane and methanol/water. The first mixture consists of non-polar fluids, while the second mixture consists of polar fluids with strong hydrogen bonding. Let us first consider the system carbon dioxide/propane. Results for AAD% in pressure P and vapor composition Y are reported for the four cases of calculations. Case (1): Since the NRTL parameters are not available from the previous calculations, τ_{12} and τ_{21} are fitted for a given α_{12}=0.3 using MPR EOS/MWS MR, for k_{ij}=0 in eqs(19) and (20). Case (2):) is fitted for the given parameters of (1). Case (3): τ_{12}, τ_{21} and k_{ij} are fitted using MPR EOS/WS MR. Case (4): Calculations are made using MPR EOS/WS MR based on the previously obtained NRTL and k_{ij} parameters due to Wong and Sandler [27]. By comparing various sets of AAD% in pressure and composition of Table 2 for the above two cases, we find that our model MPR EOS/MWS MR can predict adequately the vapor/liquid phase equilibria in carbon dioxide/propane without optimizing k_{ij} parameter, i.e., k_{ij}=0. Similar comparisons are presented for methanol/water, for which the NRTL parameters are taken from DECHEMA [35] thus leading to a true prediction. Again, MPR EOS/MWS MR is capable of describing the saturated vapor pressure and vapor composition very well. The optimization of k_{ij} leads to a slight improvement in the vapor phase composition only, which is expected.

Table 3 presents AADs% in vapor pressure and vapor composition for several mixtures investigated in this work. In general, MPR EOS/MWS MR predictions are seen to be in very good agreement with experimental data. For systems, such as

benzene/methanol, acetone/methanol, methanol/ethanol and methanol/1-butanol, MPR EOS/MWS MR results are significantly improved by optimizing k_{ij}. Although, the magnitude of k_{ij} is small, these results suggest that the difference in ionization potentials of the components and unlike interactions may be responsible for this remaining deficiency of the model.

Fig. 6 shows results for the vapor pressure as a function of the composition of carbon dioxide in carbon dioxide/propane mixture at a temperature, T=278K. Theoretical predictions are seen to be in very good agreement with experimental data over the whole range of compositions. Similar agreement between MPR EOS/MWS MR and experiment is seen in Fig.7 for another non-polar mixture ethane/hexane, at T=339K. Effect of the independent parameter k_{ij} on pressure has been also investigated. As can be seen from Fig.7, k_{ij} has no significant effect on the vapor/liquid phase equilibrium.

Fig.8 presents comparison between theoretical and experimental results for the vapor pressure of a benzene/methanol mixture. This is a highly non-ideal mixture containing an associating polar component methanol, which undergoes a significant hydrogen bonding, and a nonpolar component, benzene. The MPR EOS/MWS MR prediction agrees well with experimental data, and the azeotrope in mixture benzene/methanol is also described well.

HEAVY OIL FRACTION CHARACTERIZATION

The oil composition is determined experimentally by distillation (TBP Tests) and gas chromatography. The thermodynamic properties are calculated from the experimental information provided by the tests. A description is provided below.

True Boiling Point Tests (TBP Tests)

They are used to characterize the oil with respect to the boiling points of its components. In these tests, the oil is distilled and the temperature of the condensing vapor and the volume of liquid formed are recorded. This information is then used to construct a distillation curve of liquid volume percent distilled versus condensing

temperature. The condensing temperature of the vapor at any point in the test will be close to the boiling of the material condensing at that point. For a pure substance, the boiling and condensing temperature are exactly the same. For a crude oil the distilled cut will be a mixture of components and average properties for the cut will be determined. Table 4 shows typical results of a TBP test.

In the distillation process, the hydrocarbon plus fraction is subjected to a standardized analytical distillation, first at atmospheric pressure, and then in a vacuum at a pressure of 40 mm Hg using a fifteen theoretical plates column and a reflux ratio of five. The equipment and procedure is described in the ASTM 2892-84 book [42]. It is also common to use distillation equipment with up to ninety theoretical plates. Usually the temperature is taken when the first droplet distills over. The different fractions are generally grouped between the boiling points of two consecutive n-hydrocarbons, for example: C_{n-1} and C_n. The fraction receives the name of the n-hydrocarbon. The fractions are called hence, single carbon number (SCN). Every fraction is a combination of hydrocarbons with similar boiling points. . For each distillation cut, the volume, specific gravity, and molecular weight, among other measurements, are determined. Other physical properties such as molecular weight and specific gravity may also be measured for the entire fraction or various cuts of it. The density is measured by picnometry or by an oscillating tube densitometer. The average molecular weight of every fraction is determined by measuring the freezing point depression of a solution of the fractions and a suitable solvent, e.g., benzene.

If the distillate is accumulated in the receiver, instead of collected as isolated fractions, the properties of each SCN group cannot be determined directly. In such cases, material balance methods, using the density and molecular weight of the whole distillate and the TBP distillation curve, may be used to estimate the concentration and properties of the SCN groups [43]. A typical true boiling point curve is depicted in Figure 9. The boiling point is plotted versus the collected volume. There are several ways of calculating each fraction boiling point.

Gas Chromatography (GC)

The composition of oil samples can be determined by gas chromatography. Whilst an extended oil analysis by distillation takes many days and requires a relative large volume of sample, GC analysis can identify components as heavy as C_{80} in a matter of hours using only a small fluid sample [44]. Individual peaks in the chromatogram are identified by comparing their retention times inside the column with those on known compounds previously analyzed at the same GC conditions. The intermediate and heavy compounds are eluted as a continuous stream of overlapping compounds. This is very similar to the fractionation behavior and treated similarly. All the components detected by the GC between two normal neighboring n-paraffins are commonly grouped together, measured and reported as a SCN equal to that of the higher normal paraffin. A major drawback of GC analysis is the lack of information, such as the molecular weight and density of the different identified SCN groups. The very high boiling point constituents of an oil sample cannot be eluted, hence, they can not be analyzed by GC methods.

Thermodynamic Properties Prediction

To use any of the thermodynamic property-prediction models, e.g., equation of state, to predict the phase and volumetric behavior of complex hydrocarbon mixtures, one must be able to provide: the critical properties, temperature (T_c), pressure (P_c), acentric (ω) and molecular weight (M_w).

Petroleum engineers are usually interested in the behavior of hydrocarbon mixtures rather than pure components. However, the above characteristic constants of the pure and of the hypothetical components are used to define and predict the physical properties and the phase behavior of mixtures at any reservoir state. The properties more easily measured are normal boiling points, specific gravities, and/or molecular weights. Therefore existing correlations target these as the variables used to back up the parameters needed for EOS simulations. (T_c, P_c, ω, MW).

Many correlations of the critical properties of each pseudo-component as a function of experimentally determined variables such as; boiling point, specific gravity, average

molecular weight, have been published in literature. Whitson [4] provides an excellent review. For the sake of brevity only a brief list is include here.

Riazi and Daubert [45] developed a simple two-parameter equation for predicting the physical properties of pure compounds and undefined hydrocarbon mixtures. The proposed generalized empirical equation is based on the use of the normal boiling point and the specific gravity (γ) as correlating parameters. The basic equation is:

$$\psi = aT_b^b \gamma^c \qquad (33),$$

where T_b is the normal boiling point temperature expressed in R and the constants a, b, c, depend upon the physical property indicated by ψ. The values to calculate the pseudo-components critical properties are shown in Table 6.

Riazi and Daubert [46] modified their equation while maintaining its simplicity and significantly improving its accuracy:

$$\psi = aT_b^b \gamma^c \exp\left[dT_b + e\gamma + fT_b\gamma\right] \qquad (34)$$

$$\psi = aM_w^b \gamma^c \exp\left[dM_w + e\gamma + fM_w\gamma\right] \qquad (35).$$

The constants *a* to *f* for the two different functional forms of the correlation are presented in Table 5, and depend upon the correlated property.

Cavett [47] proposed correlations for estimating the critical pressure and temperature of hydrocarbon fractions. The correlations have received a wide acceptance in the petroleum industry due to their reliability in extrapolating at conditions beyond those of the data used in developing the correlations. The proposed correlations were expressed analytically as functions of the normal boiling point (T_b) and API gravity (γ).

Lee and Kesler [48] proposed a set of equations to estimate the critical temperature, critical pressure, acentric factor, and molecular weight of petroleum fractions. The equations use specific gravity and boiling point in ^oR as input parameters. They also proposed an equation to calculate molecular weight (M_w),

$$M_w = -12{,}272.6 + 9{,}486.4\gamma + (4.6523 - 3.3287\gamma)T_b + (1 - 0.77084\gamma - 0.02058\gamma^2)\times \left(1.3437 - \frac{720.79}{T_b}\right)\times\frac{10^{-7}}{T_b} + (1 - 0.80882\gamma + 0.02226\gamma^2)\left(1.8828 - \frac{181.98}{T_b}\right)\times\frac{10^{12}}{T_b^3}$$

(36)

Lee and Kesler [48] stated that their equations for P_c and T_c provide values that are nearly identical with those from the API Data Book up to a boiling point of 1,200°F.

Edmister [49] proposed a correlation for estimating the acentric factor ω, of pure fluids and petroleum fractions. The equation, widely used in the petroleum industry, requires boiling point, critical temperature, and critical pressure. The proposed expression is given by the following relationship:

$$\omega = \frac{3\log(P_c/14.7)}{7(T_c/T_b - 1))} - 1 \qquad (37),$$

with the temperatures expressed in degrees R.

Katz and Firoozabadi [50] presented a generalized set of physical properties for the petroleum fractions C_6 through C_{45}. The tabulated properties include the average boiling point, specific gravity; and molecular weight. The authors proposed tabulated properties are based on the analysis of the physical properties of 26 condensates and naturally occurring liquid hydrocarbons. Figure 10 shows the relationship between molecular weight and either on the normal boiling point (T_b) and API gravity (γ) according to Katz and Firoozabadi [50].

Schou Pedersen et al. [51] used extensive experimental data for seventeen North Sea oil samples obtained using high temperature chromatography. They used experimental data up to the C_{80+} fraction. They checked the validity of the equation,

$$z_n = \exp[A + B\, C_n] \qquad (38),$$

proposed by Pedersen et al. [52]. A and B are empirical constants determined by fitting the experimental data, z_n is the total molar fraction of components belonging to the fraction with n carbon number. The study found that the experimental data are well represented by Eqn. (34). Schou Pedersen et al. [51] also reported that a good representation of the heavy fraction is given by using compositional analysis up to C_{20+}.

The authors reported that there is no significant advantage increasing the accuracy of the analysis from C_{20+} to C_{80+}.

Whitson's Lumping Scheme

Whitson [53] proposed a regrouping scheme whereby the compositional distribution of Lumping is the reversed problem of splitting. The C_7+ fraction is reduced to only a few Multiple-Carbon-Number (MCN) groups. Whitson suggested that the number of MCN groups necessary to describe the plus fraction is given by the following empirical rule:

$$N_g = Int[1 + 3.3\log(N - n)] \quad (39), \text{ where:}$$

N_g = number of MCN groups

Int = Integer

N = number of carbon atoms of the last component in the hydrocarbon system

n = number of carbon atoms of the first component in the plus fraction

The integer function requires that the real expression evaluated inside the brackets be rounded to the nearest integer. The molecular weights separating each MCN group are calculated from the following expression:

$$Mw_I = Mw_n\left[\exp\left[\frac{1}{N_g}\ln\left(\frac{Mw_N}{Mw_n}\right)\right]\right]^I \quad (40),$$

where Mw_N = molecular weight of the last reported component in the extended analysis of the plus fraction and Mw_n = molecular weight of the first hydrocarbon group in the extended analysis of the plus fraction.

I = 1, 2,..., N_g

Molecular weight of hydrocarbon groups (molecular weight of C_7-group, C_8-group, etc.) falling within the boundaries of these values are included in the I^{th} MCN group.

A sample calculation is shown in Table 6. The molecular weight of fraction 1 is 96 while the molecular weight of fraction 45 is 539. The method predicted 6 pseudo-fractions with the molecular weights shown in the Table. The components with molecular weights between pseudo-components k-1 and k are ascribed to pseudo-component k. Complete calculations for several oil samples are presented in the Appendix.

RESULTS AND DISCUSION

EXPERIMENTAL RESULTS

Evaluation of Bubble Point Pressures

Bubble Point Pressure for Crude Oil (A) and of this crude oil with Methane and Water, have been measured in the range 212-315 ^{o}F (100 175 ^{o}C). The result gives us a very good idea about what happens in a reservoir while injecting the water or steam for Enhanced Oil Recovery, especially the change in the bubble point pressure which is an important variable for oil production.

The objective of this study is to calculate bubble pressures for the several oil samples aforementioned. We also want to know the influence of the water injection on the value of the bubble point pressure at the conditions of reservoir and to find the relation between the quantity of water added to the reservoir and the amount of pressure reduced from the bubble point.

Figures 11 to 14 show the isothermal pressure volume behavior of some of these oils (A-D). Bubble point pressures were determined by least square regression of the two curves indicating liquid phase and two-phase regions. Table 7 indicates the differences in bubble point pressures obtained for all these experiments. The purpose of adding methane was to be able to detect the bubble point pressure experimentally. Equations of state predicting two phase equilibria, rather than three phase equilibria, predict a substantial increase in the bubble point pressure of an oil when water is added. This is mainly an artifact of predicting two phase equilibria instead of three-phase equilibria.

The experiments for oils E and F resulted mostly in P-V plots similar to the 100 ^{o}C curve in Fig. 11. This behavior indicates that the bubble point occurs at temperatures above the experimental limit for our apparatus or at saturation pressures below 14.7 psi. Our computer results confirm this conclusion and are shown in the next section. The points where a determination was done are also listed in Table 7.

PHASE EQUILIBRIUM RESULTS

Synthetic Mixtures

We have performed several calculations for mixtures consisting of non-polar, non-associating polar and associating polar fluids. However, we present here results for a few selected binary mixtures and multicomponent mixtures only. We also include some results from the van der Waals mixing rules as appropriate for the comparison with MWS MR. Since the details of the predictive power of this kind of approach has already been presented earlier using a similar form of MPR EOS (Fotouh and Shukla, [34]), those results are not repeated here.

Table 8 reports results for the absolute average deviation between experimental and calculated results of saturated vapor pressures and vapor mole fractions for 13 binary mixtures. In general, calculations based on MWS MR are more accurate than those using VDW MR, in particular for nonideal mixtures. Also, in some mixtures MWS MR results are more accurate than WS MR results. The advantage of MWS MR over WS MR is that the unlike energy interaction parameters of MWS MR are relatively smaller in magnitude than those of the latter. Therefore, MWS MR can describe vapor-liquid equilibria of many mixtures even without using the unlike interaction energy parameter.

Now, we present results for a three-component mixture acetone/methanol/water, in which the first component is non-associating polar fluid and other two components are highly associating polar fluids. In Table 9, the MPR EOS/MWS MR results for the vapor pressure and vapor mole fraction compare well with experimental data. The predictions based on MPR EOS/MWS MR model are seen to be more accurate than those based on either VDW MR or WS MR. Similar comparisons are seen in Table 10 for nitrogen/carbon dioxide/propane mixture, in which the first two components are nonpolar

nonhydrocarbon fluids while the third component is a hydrocarbon fluid.

Finally, we illustrate the performance of our model for two selected multicomponent mixtures consisting of 11 and 12 components. Table 11 presents comparison between calculated results and experimental data of vapor pressure and vapor phase compositions of the components. Results from both MPR EOS/VDW MR and MPR EOS/MWS MR models are almost equivalent for these mixtures. Nevertheless, these comparisons suggest that the MPR EOS combined with MWS MR is a very reliable model for the prediction of phase equilibria even in multi-component mixtures of reservoir interest.

Oil Samples

We used Whitson [53] technique to characterize several oil samples collected from literature and obtained from Bio-Engineering Inc. and other sources. A complete list including compositional information and results is presented in the Appendix. The procedure used involved the following steps:

1. Data corresponding to maximum and minimum carbon numbers and molecular weights were collected. Normally we used 20 as the maximum carbon number and 7 as the minimum. Some runs were done using 30 and 80, but the results did not differ significantly from using 20. Schou Pedersen et al. [51] reported similar conclusions.

2. A computer program was developed to implement Whitson [53] method using eqn. (39) to calculate the number of pseudo-components and eqn. (40) to calculate the limits between them.

3. The carbon number fractions in between the calculated limits were lumped together. Molecular weights, specific gravities and molar fractions were calculated for the different pseudo-components using the set of equations reported by Whitson [4].

4. The general equation proposed by Riazi and Daubert [46], equation (35), with the data presented in Table 5 was used to calculate critical temperatures (T_c),

pressures (P_c) and volume (V_c). The same equation was also used to calculate saturated boiling temperature (T_b).

5. Edminster equation, eqn. (37), was used to calculate the Pitzer acentric factor.

6. Wilson and Sandler [29] mixing rules, eqns. (21) and (24), were used to calculate the pseudo-components thermodynamic properties.

After these calculations we have a complete set of data to be used in our P-V-T programs. Two programs were developed to calculate, bubble point and dew point saturation pressures using the modified Peng-Robinson EOS [34] and several mixing rules (vDW, WS, MWS MR). In both cases the program provides the saturation point pressure plus the vapor-liquid equilibrium compositions. The bubble point pressure program can be used to simulate our P-V experiments.

Our dew point calculation program was used to predict the values reported by Eilerts et al. [64]. The authors reported experimental values for the OO-L-544 fluid. This fluid is a gas condensate containing 90.162 mol% methane and 1.51 mol% C_7^+ fraction. The C_7^+ fraction has a molecular weight of 167.3 and specific gravity of 0.8051. Fractional distillation data are available up to C_{24}. The compositional information was converted into single carbon groups using the method reported by Whitson [53] and the procedure reported above to calculate the thermodynamic properties of the pseudo-components.

Predicted dew pressures for three constant temperatures; 300, 350 and 400 K, are shown in Table 12. There is very good agreement between our predictions and experimental data.

Table 13 shows a comparison between the experimental and calculated bubble point pressures for different constant temperatures. We can see that the calculated results using the oil compositions depicted in the Appendix agree well with the experimental data. The calculated results also predict correctly the increase of saturation pressure as temperature increases.

Table 14 shows a comparison among the oils A, E and F. The bubble pressure increases as the temperature increases. The oil samples richer in the less volatile component require less pressure to reach the saturation condition.

Tables 15 to 18 show calculations done using several oil samples, A, E and F. In all cases values of vapor phase molar fractions in equilibrium with a single liquid composition are presented for different temperatures. The numerical calculations reproduce our experiments. Oils A, E and F vary in composition and physical properties. Tables 15, 16 and 17 present vapor-liquid equilibrium data for pure oil samples. The results presented in Table 18 were calculated using a mixture of oil A with 20 g of methane and 5 g of water. This mixture was called, oil G. The number of moles of the added compounds was calculated and calculation of the new molar fractions was done. The complete composition of oil B is presented in the Appendix. The values of all the saturation pressures were included in the tables. Inspection of the results presented in Table 18 shows that the calculated bubble pressures differ considerable from the corresponding experimental results. The reason is the presence of two immiscible liquid phases. The simulator used in this work is a two phase (vapor-liquid) one, therefore, cannot capture the presence of the second liquid phase. It operates under the assumption that all the water present is dissolved into the organic phase. This assumption contradicts experimental results (Barrufet and Rahman [10]).

CONCLUSIONS

A modification of the Peng-Robinson equation of State (MPR EOS) has been developed. This modification involves improved calculations of the volume translation term. A theoretically consistent modification of the Wong and Sandler mixing rules has also been implemented (MWS MR). The combination of the modified EOS and the improved mixing rules have been implemented in a process that allows calculations of P-V-T behavior for fluid mixtures of interest in the oil industry. We have validated extensively the modified EOS and the new mixing rules (MWS MR) determining phase equilibria and physical properties of single components and binary and multicomponent mixtures. Polar fluids, non-polar fluids and mixtures of both have been used to verify the accuracy of the proposed procedure. Comparisons of the proposed mixing rules against similar ones have shown an improvement in the accuracy of the calculated phase

equilibrium diagrams. The proposed procedure has been successfully applied to multicomponent mixtures even in presence of nitrogen, carbon dioxide and water. Good agreement with reported vapor-liquid phase equilibrium data has been found.

A technique has been proposed to represent complex reservoir fluids. The composition of the oil samples is represented by the C_1, C_2, C_3, C_4, C_5, and C_6 fractions plus several pseudo-components obtained by splitting and lumping the C_7^+ fraction. The procedure developed by Whitson [53] allows straightforward calculation of the pseudo-components. Riazi and Daubert [46] equations are used to compute the critical properties while Edminster [49] equation is used to compute the Pitzer acentric factor. This procedure provides all the required information to be entered into thermodynamic simulators.

P-V-T behavior was studied using bubble and dew point computer programs based upon the modified Peng-Robinson equation and the improved mixing rules. We also conducted P-V-T experiments with several oil samples. We were able to reproduce successfully the experimental results obtained with pure oil samples. Our simulators were able to predict successfully the saturation pressure at constant temperature. They also reported the composition at equilibrium of the vapor and liquid phases. Successful agreement between computed and experimental vapor-liquid equilibrium data was achieved in the cases where experimental information was available. This agreement applied even to mixtures of twelve components involving nitrogen, carbon dioxide and water. Our simulators were not successful in predicting the presence of more than two phases in the experimental device. This is a common problem that two phases simulators face. The problem of water solubility in oil and the significant influence of this phenomenon on phase equilibrium prediction is a current research subject.

In conclusion we have developed a complete technique to calculate phase equilibrium behavior of complex reservoir fluids. Our extensive results suggest that this technique can be confidently incorporated into commercial simulators.

NOMENCLATURE

a	Energy parameter
A_{jk}	Coefficients of eqn, (12)
A_{∞}^{E}	Excess Helmholtz free energy
b	Excluded-volume parameters
B_{ij}^{ex}	Experimental cross second virial coefficient
F_c	Additional volume correction term
G^E	Excess Gibbs free energy
I_i	Ionization potential of component i.
k_{ij}	Interaction second virial coefficient parameter eqn. (25)
P	Pressure
P_c	Critical pressure
R	Gas constant
T	Absolute temperature
T_b	Normal boiling point
T_c	Critical temperature
v	Molar volume
V_c	Critical volume
X	Parameter of α-term Eqn.(8)
z_n	molar fraction with n carbon number
Z	Compressibility factor

Greek Symbols

α	α-term
α_{12}	NRTL parameter
γ	Specific gravity
ϕ	Fugacity Coefficient
σ	Constant eqn. (21)ED
τ_{12}	NRTL parameter
ω	Acentric factor

Abbreviations

EOS	Equation of state
MPR EOS	Modified Peng-Robinson EOS
MWS MR	Modified Wilson mixing rule
PR EOS	Peng-Robinson EOS
vDW MR	van Der Waals mixing rule
WS MR	Wilson mixing rule

REFERENCES

[1] T.G. Harding, T.G., S.M. Farouq Ali, and D.L. Flock, Steamflood Performance in the Presence of Carbon Dioxide and Nitrogen, J. Cdn. Pet. Tech. (Sept. - Oct. 1983) 30-37.

[2] E. A. Turek, R.S. Metcalfe, L. Yarborough and R.L. Robinson, Jr., "Phase Equilibria in Carbon Dioxide-Multicomponent Hydrocarbon Systems: Experimental Data and an Improved Prediction Technique", SPE J. **24**, 308 (1984).

[3] Shukla, K. and Gabitto, J. F. “Improved Peng-Robinson Equation of State for Mixtures of Heavy Hydrocarbons”, submitted for publication to Fluid Phase Equilibria, 2002.

[4] Whitson, C., "Characterizing Hydrocarbon Plus Fractions," Paper EUR 183, presented at the *European Offshore Petroleum Conference* held in London, October 21-24, 1980.

[5] Wu, C. H. A Critical Review of Steamflood Mechanisms, SPE 6550, presented in the 47th SPE Annual California Regional Meeting, Bakersfield, California, 1977.

[6] McKetta, J.J., Jr. and Katz, D.L.: "Phase Relations of Hydrocarbon-Water Systems," Trans. AIME (1947) v.170, p.34.

[7] Mehra, R.K., Heidemann, R.A. and Aziz, K.: "Computation of Multiphase Equilibrium for Compositional Simulation," Soc. Pet. Eng. J. (1982) 61-68.

[8] Shibata, S.K. and S.I. Sandler, "High-Pressure Vapor-Liquid Equilibria of Mixtures of Nitrogen, Carbon Dioxide and Cyclohexane", J. Chem. Eng. Data. 34, 419 (1989).

[9] Lansangan, R.M., and Smith, J.L.: “Viscosity, Density and Composition Measurements of CO_2/West Texas Oil System,” SPE Reservoir Eng., 8, 1993.

[10] Barrufet, M.A., and Rahman, S.: “A New Technique for Simultaneous Measurement of PVT and Phase equilibrium Properties of Fluids at High temperatures and Pressures,” *Petroleum Science and Engineering*, 14, (1995).

[11] Boberg, T. C., Thermal Methods of Oil Recovery, New York (1988).

[12] Hornbrook, M.W., Dehghani, K., Qadeer, S., and Ostermann, R.D.: "Effects of CO_2 Addition to Steam on Recovery of West Sak Crude Oil," SPERE (August 1991) 278-286.

[13] van der Waals, J. D., Ph.D. Dissertation, Leiden (1873).

[14] Weng, W.L. and M.J. Lee, "Vapor-Liquid Equilibrium of the Octane/Carbon Dioxide, Octane/Ethane and Octane/Ethylene Systems", J. Chem. Eng. Data **37**, 213 (1992).

[15] Peng, D. Y. and Robinson, D. B., "A New Two-Constant Equation of State", Ind. Eng. Chem. Fundam., **15** (1976) 59.

[16] Anderko, A., "Equation of State Methods for the Modeling of Phase Equilibria", Fluid Phase Equilib., **61** (1990) 145.

[17] Sandler, S. I., Orbey, H. and Lee, B.-I., "Equations of State, in Models for Thermodynamic and Phase Equilibrium Calculations", ed. S.I. Sandler, Marcel Dekker, New York, **ch.3** (1994).

[18] Economou, I. G. and Donohue, M. D., "Equations of State for Hydrogen Bonding Systems", Fluid Phase Equilib., **116** (1996) 518.

[19] Fotouh, K. and Shukla, K., "An Improved Peng-Robinson Equation of State with a New Temperature Dependent Attractive Term", Chem. Eng. Commn., **159** (1997) 209-229.

[20] Raal, J. D., and Muhlbauer, A. L., "Phase Equilibria: Measurement and Computation", Taylor and Francis, London (1998).

[21] Sandler, S. I., Chemical Engineering Thermodynamics. Third Edition, John Wiley and Sons, New York (1999).

[22] Wei, Y. S., and Sadus, R. J., "Equations of State for the Calculation of Fluid Phase Equilibria", AIChE Journal, **46** (2000) 169.

[23] Twu, C. H., Coon, J. E. and Cunningham, J. R., "A New Generalized Alpha Function for a Cubic Equation of State. Part 2. Redlich-Kwong Equation", Fluid Phase Equilib., **105** (1995) 61.

[24] Leibovici, C. F., "A Unified m(ω) Relation for Cubic Equations of State", Fluid Phase Equilib., **101** (1994) 1.

[25] Mathias, P. M., Naheiri, T. and Oh, E. M., “A Density Correction for the Peng-Robinson Equation of State,” Fluid Phase Equilib., **47** (1989) 77.

[26] Graboski, M.S. and Daubert, T.E., “A Modified Soave Equation of State for Phase Equilibrium Calculations,” Ind. Eng. Chem. Process Des. Dev., **17** (19780 443.

[27] Sandler, S.I., Orbey, H. and Lee, B.-I. Equations of State, in Models for Thermodynamic and Phase equilibrium calculations. ed., S.I. Sandler, Marcel Dekker, New York, ch.3 (1994).

[28] Huron, M.J. and Vidal, J. New Mixing Rules in Simple Equation of State for Representing Vapor-Liquid Equilibria of Strongly Nonideal Mixtures. Fluid Phase Equilib., **3**, (1979) 255.

[29] Wong, D.S. and Sandler, S.I. Theoretically Correct New Mixing Rule for Cubic Equations of State. AIChE J., **38**, (1992) 671.

[30] Wong, D.S.H., Orbey, H. and Sandler, S.I. Equation of State Mixing Rule for Nonideal Mixtures Using Available Activity Coefficient Model Parameters and That Allows Extrapolation Over Large Ranges of Temperature and Pressure. Ind. Eng. Chem. Res., **31**, (1992) 2033.

[31] Orbey, H, Sandler, S.I. and Wong, D.S.H. Accurate Equation of State Predictions at High Temperatures and Pressures using the Existing UNIFAC Model. Fluid Phase Equilib., **85**, 91993) 41.

[32] Huang, H. and Sandler, S.I. Prediction of Vapor/Liquid Equilibria at High Pressures Using Activity Coefficient Parameters Obtained from Low Pressure Data: A comparison of Two Equations of State Mixing Rules. Ind. Eng. Chem. Res., **32**, (1993) 1498.

[33] Eubank, P.T., Shyu, G.-S. and Hanif, N.S.M. New Procedures for Application of the Wong-Sandler Mixing Rules to the Prediction of Vapor-Liquid Equilibria. Ind. Eng. Chem. Res., **34**, (1995) 314.

[34] Fotouh, K. and Shukla, K. Prediction of Phase Equilibria in Binary Mixtures using an Improved Equation of State and Theoretically Consistent Mixing Rule. Chem. Eng. Commn., **166**, 35 (1998).

[35] Gmehling, J. and Onken, U. DECHEMA Chem. Data Ser., Vol. I, Pt. 1, P.42, 49 (1977).

[36] Shukla, K. Vapor-Liquid Equilibria and Thermodynamic Properties of Molecular Fluids.II. Binary Fluid Mixtures, Fluid Phase Equilib., **99**, 153 (1994).

[37] Gray, C.G. and Gubbins, K.E. Theory of Molecular Fluids. Clarendon Press, Oxford (1984).

[38] Renon, H. and Prausnitz, J.M. "Local Compositions in Thermodynamic Excess Functions for Liquid Mixtures," AIChE J., **14**, 135 (1968).

[39] Reamer, H.H., Sage, B.H. and Lacey, W.N. Phase Equilibria in Hydrocarbon Systems: Volumetric and Phase Behavior of the Propane-Carbon Dioxide System. Ind. Eng. Chem. **43**, 2515 (1951).

[40] Knapp, H., Doring, R., Oellrich, L., Plöcker, U. and Prausnitz, J.M., DECHEMA Chem. Data Ser., Vol. VI, P.557 (1982).

[41] Gmehling, J., Onken, U. and Arlt, W. DECHEMA Chem. Data Ser., Vol. I, Pt. 2c, P.59, 73-77, 126-127, 178 (1982).

[42] ASTM, "Distillation of Crude Petroleum, Designation D2892-84," *Annual Book of ASTM Standards*, (1984) 821-860.

[43] Hernandez, M. J. and Casrells, F. "A New Method for Petroleum Fractions and Crude Oil Characterization," *SPE Reservoir Engineering* (1992) 265-270.

[44] Curvers, J. and van den Engel, P. "Gas Chromatographic Method for Simulated Distillation up to a Boiling Point of 750 oC Using Temperature-Programmed Injection and High Temperature Fused Silica Wide-Bore Columns," *J. High Resolution Chromatography*, (1989) **12**, 16-22.

[45] Riazi, M. R. and Daubert, T. E. "Simplify Property Predictions," *Hydrocarbon Proc.* (1980) **59(3)**, 115-116.

[46] Riazi, M. R. and Daubert, T. E. "Characterization Parameters for Petroleum Fractions," *Ind. Eng. Chem. Research* (1987) **26**, 755-759.

[47] Cavett, R. H. "Physical Data for Distillation Calculations, Vapor-Liquid Equilibria," *Proc. Of 27th API Meeting*, San Francisco (1962) 351-366

[48] Lee, B. I. And Kesler M. G. "Improve Vapor Pressure Prediction," *Hydrocarbon Proc.*, (July 1980) 163-167.

[49] Edminster, W. C. "Applied Hydroccarbon Thermodynamics Part 4: Compressibility Factors and Equations of State," *Pet. Refiner*, (April 1958), **37**, 173-79.

[50] Katz, D. L. and Firoozabadi, A. "Predicting Phase Behavior of Condensate/Crude Oil Systems Using Methane Interaction Coefficients," *JPT*, (1978) 1649-55.

[51] Schou Pedersen, K., Blilie, A. L. and Meisinget, K. K. "PVT Calculations on Petroleum Reservoir Fluids Using Measured and Estimated Compositional Data for the Plus Fraction," *Ind. Eng. Res*., (1992) **31**, 1378-1384.

[52] Pedersen, K. S., Thomassen, P., and Fredenslund, As. "Characterization of Gas Condensates Mixtures," *Adv. Thermodyn*., (1989b) **1**, 137-148.

[53] Whitson, C., "Characterizing Hydrocarbon Plus Fractions," *Soc. Of Pet. Engineers Journal*, (August 1983), **37**, 683-694.

[54] Niesen, V. "Vapor-Liquid Equilibria and Coexisting Densities of CO2-n-Butane at 311 to 395K." *J. Chem. Thermodyn*., **21**, 915 (1989).

[55] Besserer, G. and Robinson, D.B. "Equilibrium Phase Properties of n-Pentane-Carbon Dioxide System." *J. Chem. Eng. Data*, **18**, 417 (1973).

[56] Li, Y-H, Dillard, K.H. and Robinson, Jr., R.L. "Liquid-Vapor Equilibrium for Carbon Dioxide-n-Hexane at 40, 80 and 120 ^{o}C." *J. Chem.. Eng. Data*, **20**, 53 (1981).

[57] Sebastian, H., Simnick, J., Lin, H-M, and Chao, K.C. "Vapor Liquid Equilibria in Binary Mixtures of Carbon Dioxide-n-Decane and Carbon Dioxide-n-Hexadecane." *J. Chem. Eng. Data*, **25**, 138 (1980).

[58] Shah, N.N., Zollweg, J.A. and Streett, W.B. "Vapor-Liquid Equilibrium in the System Carbon Dioxide+Cyclopentane from 275 to 493 K at Pressures to 12.2 MPa." *J. Chem. Eng. Data*, **36**, 188 (1991).

[59] Kahre, L.C. "Low Temperature K data for Methane-n-Pentane." *J. Chem. Eng. Data*, **20**, 363 (1975).

[60] Verhoeye, L. and Schepper, H. "The Vapor-Liquid Equilibria of the Binary, Ternary and Quarternary Systems Formed by Acetone, Methanol, Propan-2-ol and Water." *J. Appl. Chem. Biotechnol*., **23**, 607 (1973).

[61] Kurihara, K., Hori, H. and Kojima, K. "Vapor-Liquid Equilibrium Data for Acetone-Methanol-Benzene, Chlorform-Methanol-Benzene and Constituent Binary Systems at 101.3 Kpa." *J. Chem. Eng. Data*, **43**, 264 (1998).

[62]. Kato, M., Sato, T., Konishi, H. and Hirata, M. "Measuring Ternary Vapor-Liquid Equilibria. Dew, Bubble and Condensation Point Method." *J. Chem. Eng. Jpn*., **4**, 311 (1971).

[63] Yucelen, B. and Kidnay, A.J. "Vapor-Liquid Equilibria in the Nitrogen+Carbon Dioxide+Propane System from 240 to 330K at Pressures to 15Mpa." *J. Chem. Eng. Data*, **44**, 926 (1999).

[64] Eilerts C. K. et al. "Phase Relations of a Gas-Condensate Fluid at Low Temperatures, Including the Critical State." *Pet. Eng.*, 154-180, (Feb. 1948).

TABLES

Table 1. Volume translation parameters and percentage deviation between experimental and calculated results for saturated liquid (L) and vapor (V) densities.

Fluid	N_p	S1	S2	AAD%(L)	AAD%(V)
Methane	22	4.7931	0.41	0.5	1.3
Ethane	18	5.0711	0.41	1.2	1.4
Propane	21	5.4937	0.41	1.4	2.4
Butane	25	5.6073	0.41	1.5	2.7
Pentane	27	4.4819	0.41	1.3	-
Hexane	26	2.9489	0.41	1.2	-
Heptane	28	0.7225	0.41	1.3	-
Octane	28	-1.9000	0.41	1.5	-
Nonane	26	-2.8361	0.41	1.5	-
Decane	17	-2.0389	0.41	2.6	-
Undecane	18	-7.4421	0.41	4.7	-
Dodecane	18	-13.7956	0.41	2.5	-
Tridecane	16	-11.6188	0.41	4.0	-
Tetradecane	18	-21.7151	0.41	2.5	-
Pentadecane	17	-15.2657	0.41	4.0	-
Hexadecane	18	-31.4161	0.41	4.5	-
Heptadecane	19	-38.3081	0.41	4.4	-
Octadecane	19	-76.0498	0.41	2.1	-
Nonadecane	18	-92.3445	0.41	2.9	-
Eicosane	20	-112.9399	0.41	2.4	-
Propene	23	6.2970	0.41	1.1	0.9
Benzene	30	3.1684	0.41	1.3	5.22
Toluene	28	-11.3182	0.41	4.9	-
H_2	19	5.9619	0.41	0.8	1.4
CO_2	46	2.3996	0.41	0.5	2.2
Kr	22	4.2314	0.41	1.0	2.4
H_2O	24	-3.4501	0.41	1.5	1.2
O_2	31	3.6736	0.41	1.0	1.2

Table 2. Results for vapor pressure and vapor phase composition using MPR EOS/MWS MR.

System	T, K	α_{12}	τ_{12}	τ_{21}	k_{ij}	N_p	AAD%		Method
							P	Y	
carbon dioxide/ propane	277.6	0.3	2.4223	0.1800	0	10	0.33	1.05	CR
		0.3	2.4223	0.1800	0.0001	10	0.33	1.05	CR
		0.3	3.8405	0.6512	0.0174	10	1.30	3.31	WS
		0.3	1.2600	-0.1800	0.3730	10	2.48	2.75	WS
methanol/water	298.2	0.3	-0.1662	0.6462	0	9	3.41	2.20	CR
		0.3	-0.1662	0.6462	0.0261	9	3.58	1.93	CR
		0.3	-0.1662	0.6462	0.0555	9	5.10	5.40	k_{12}-fit
		0.3	-0.1187	0.6512	0.0423	9	4.78	4.95	3p-fit
	373.2	0.3	-0.5442	1.5017	0	12	1.47	4.06	CR
		0.3	-0.5442	1.5017	0.1104	12	1.13	3.76	WS

Table 3. Comparison of vapor pressure and vapor phase composition from MPR EOS/MWS MR$^+$ and experiment

System	T, K	α_{12}	τ_{12}	τ_{21}	$k_{ij} = 0$			k_{ij} ++	
					ΔP%	ΔY%	k_{ij}^{++}	ΔP%	ΔY%
carbon dioxide/ propane[1]	278	0.3	2.4261	0.1779	0.3	1.1	0.0001	0.3	1.1
ethane/hexane[2]	339	0.3	3.9141	-1.8886	2.9	0.9	-0.0328	1.8	0.9
butane/methanol[3]	323	0.3	0.9607	4.4623	1.3	6.6	-	-	-
benzene/methanol[4]	308	0.3	1.1497	1.9717	8.2	2.4	0.1536	0.6	3.3

acetone/methanol[5]	298	0.3	1.2214	-0.5071	5.5	0.5	0.1271	1.2	5.7
	308	0.3	1.5250	-0.6521	5.5	0.9	0.1265	1.3	5.5
methanol/ethanol[6]	298	0.3	-0.0613	0.0262	4.3	2.7	0.0765	1.8	1.6
methanol/1-butanol[7]	298	0.248	1.3406	-0.8213	6.8	0.9	0.1062	2.4	0.1
methanol/water[8]	298	0.3	-0.1662	0.6462	3.4	2.2	0.0261	3.5	1.9
	373	0.3	-0.5442	1.5017	1.5	4.1	0.0350	1.1	3.7
ethanol/water[9]	298	0.036	-2.2597	3.9679	2.4	3.9	0.0300	1.6	1.5

In most cases, NRTL parameters are taken from DECHEMA. Otherwise, for a fixed α_{12}, NRTL parameters τ_{12} and τ_{21} are determined by minimizing the error in the objective function. 1-9 taken from literature.

Table 4. Typical results for a TBP test.

Component	Ti	Tf	T mean	ΔV (cm3)	Σ(ΔV)	V % Off
Hypo1	99	220	*159.5*	5.1	*5.1*	*5.3*
Hypo2	214	323	*268.5*	8.0	*13.1*	*13.5*
Hypo3	323	432	*377.5*	7.9	*21.0*	*21.7*
Hypo4	432	526	*479*	8.1	*29.1*	*30.1*
Hypo5	526	612	*569*	7.9	*37.0*	*38.2*
Hypo6	612	693	*652.5*	7.9	*44.9*	*46.4*
Hypo7	693	765	*729*	7.9	*52.8*	*54.5*
Hypo8	765	821	*793*	7.8	*60.6*	*62.6*
Hypo9	821	908	*864.5*	8.1	*68.7*	*71.0*
Hypo10	908	1010	*959*	5.2	*73.9*	*76.3*
Residual			***1261.1692***	*22.9*	*96.8*	*100.0*
Whole Oil			*729*			
Residual Volume Left				*22.9*		

Table 5. Parameters for Riazi and Daubert [46] (Eqns. (34) and (35)).

Form (1)				
Constant	***Mw***	***Tc (^oR)***	***Pc (psia)***	***Vc (ft^3 / lbm)***
a	581.96	10.6443	6.162×10^{6}	6.233×10^{-4}
b	0.97476	0.81067	-0.4844	0.7506
c	6.51274	0.53691	4.0846	-1.2028
d	5.43076×10^{-4}	-5.1747×10^{-4}	-4.725×10^{-3}	-1.4679×10^{-3}
e	9.53384	-0.54444	-4.8014	-0.26404
f	1.11056×10^{-3}	3.5995×10^{-4}	3.1939×10^{-3}	1.095×10^{-3}
Form (2)				
Constant	***Tc (^oR)***	***Pc (psia)***	***Vc (ft^3 / lbm)***	***Tb (^oR)***
a	544.4	4.5203×10^{-4}	1.206×10^{-2}	6.77857
b	0.2998	-0.8063	0.20378	0.401673
c	1.0555	1.6015	-1.3036	-1.58262
d	-1.3478×10^{-4}	-1.8078×10^{-4}	-2.657×10^{-3}	3.77409×10^{-3}
e	-0.61641	-0.3084	0.5287	2.984036
f	0.0	0.0	2.6012×10^{-3}	-4.25288×10^{-3}

Table 6. Grouping data for characterization of fractions with up to 45 components.

Group	Molecular Weight
1	127
2	170
3	227
4	303
5	404
6	539

Table 7. Bubble Point Pressure at Bubble Point point for crude oils A to F.

Temp. (oC)	Oil A	Oil B	Oil C	Oil D	Oil E	Oil F
100	< 14.7	2108	2079	2062	-	-
125	36	2123	-	-	-	-
150	45	2156	2179	2169	-	-
175	62	2186	2249	2185	18.5	18

Table 8. Results for some selected binary mixtures

Mixture	T (K)	P(bar)	MR	τ_{12}	τ_{21}	k_{12}	ΔP%	Δy%
CO_2-Propane[1]	344	28-58	VDW WS MWS	- 10.6703 1.4096	- 0.4098 -0.1231	0.1539 0.4360 0.1363	0.5 1.1 0.2	2.3 2.2 1.5
CO_2-Butane[2]	378	16-74	VDW WS MWS	- 8.3764 1.1847	- -0.0521 -0.2687	0.1368 0.3911 0.1127	0.9 0.7 0.8	1.6 3.5 1.2
CO_2-Pentane[3]	344	4-91	VDW WS MWS	- 10.6703 1.8977	- 0.4098 -0.4142	0.1303 0.4360 0.0560	2.9 1.1 0.6	1.4 2.2 1.1
CO_2-Hexane[4]	313	8-75	VDW WS MWS	- 1.7778 2.4251	- -0.0406 -0.2729	0.1205 0.1855 0.0417	2.2 2.1 0.8	0.3 0.1 0.1
CO_2-Decane[5]	462	19-51	VDW WS MWS	- 3.9161 1.1729	- -0.1090 -1.0072	0.0134 0.0989 0.0989	0.7 1.0 1.3	0.5 9.2 0.5
CO_2-Hexadecane[6]	463	20-51	VDW WS MWS	- 1.2212 1.0200	- 0.0075 -1.0012	-0.0571 0.2364 0.1014	0.6 1.3 1.8	0.1 3.2 0.2
CO_2-Cyclopentane[7]	313	3-79	VDW WS MWS	- 9.4436 1.6198	- 0.7833 0.0273	0.1292 0.3343 0.0900	3.8 2.7 0.9	0.7 0.9 0.8
Acetone-Methanol[8]	298	0.1-0.3	VDW WS MWS	- 1.1309 0.9348	- -0.3653 -0.1572	-0.0063 0.1251 0.0485	3.6 1.6 0.3	6.7 3.3 1.0
Methane-Pentane[9]	283	6-152	VDW WS MWS	- 9.8650 1.4913	- 0.0718 -1.0494	-0.1155 0.1000 -0.4850	7.9 9.0 1.5	0.4 10.4 1.5
Methanol-Benzene[10]	293	0.1-0.13	VDW WS MWS	- 2.6167 2.1007	- 1.1040 0.7535	0.0739 0.0833 0.1680	2.2 2.6 2.2	4.5 1.2 1.2
Methanol-Water[11]	373	1-3	VDW WS	- 0.3200	- 0.0988	-0.0863 0.0999	1.1 2.0	2.0 0.7

			MWS	0.0695	0.0996	0.1000	1.1	0.4
Acetone-Water[12]	373	1-4	VDW WS MWS	- 0.9128 0.9341	- 1.3046 0.8676	-0.1994 0.2916 0.1755	13 1.8 1.8	24 2.5 2.0
Acetone-Benzene[13]	298	0.1-0.4	VDW WS MWS	- 0.2529 0.2287	- 0.1027 0.0955	0.0282 0.1002 0.1004	1.7 1.7 1.6	2.1 1.9 1.9
Ethane-Hexane[14]	339	2-62	VDW WS MWS	- -1.1240 -1.2887	- 0.6504 0.9719	-0.0039 0.3952 -0.0086	10.9 1.3 1.2	1.4 1.0 0.9

[1][39], [2][54], [3][55], [4][56], [5][57], [6][57], [7][58], [8][41], [9][59], [10][41], [11][35], [12][60], [13][61], [14][40].

Table 9. Results for a ternary mixture, acetone/methanol/water at 523K+

Set N°	T (K)	P(bar) ex	P(bar) VDW	P(bar) WS	P(bar) MWS	
1	523	62.06	52.696	53.568	60.940	
2	523	58.48	51.125	50.926	57.305	
3	523	52.89	47.500	46.224	50.523	
Set N°	Component	X(ex)	Y(ex)	Y(VDW)	Y(WS)	Y(MWS)
1	1	0.1370	0.2370	0.1801	0.2224	0.2828
	2	0.0940	0.1480	0.1533	0.1546	0.1512
	3	0.7690	0.6150	0.6666	0.6229	0.5661
2	1	0.0880	0.1920	0.1377	0.1628	0.2238
	2	0.0840	0.1450	0.1518	0.1538	0.1549
	3	0.8280	0.6630	0.7105	0.6834	0.6212
3	1	0.0430	0.1430	0.0964	0.0978	0.1492
	2	0.0490	0.0950	0.1098	0.1059	0.1119
	3	0.9080	0.7620	0.7938	0.7963	0.7389

+Experimental data are from Kato et al. [62].

Table 10. Results for a ternary mixture, nitrogen/carbon dioxide/propane at 270K[+]

Set N[o]	T (K)	P(bar) Exp.	P(bar) VDW	P(bar) WS	P(bar) MWS	
1	270	20	17.936	18.505	18.800	
2	270	60	61.806	53.503	59.566	
3	270	130	129.560	127.310	129.865	
Set N[o]	Component	X(exp.)	Y(exp.)	Y(VDW)	Y(WS)	Y(MWS)
1	1	0.0286	0.6812	0.6592	0.6282	0.6679
	2	0.0182	0.0676	0.0528	0.0598	0.0539
	3	0.9532	0.2512	0.2888	0.3120	0.2783
2	1	0.1012	0.5894	0.5955	0.4768	0.5783
	2	0.3038	0.2935	0.2879	0.3344	0.3038
	3	0.5950	0.1171	0.1171	0.1888	0.1179
3	1	0.2663	0.8386	0.8521	0.7439	0.8614
	2	0.0217	0.0192	0.0169	0.0307	0.0169
	3	0.7120	0.1423	0.1310	0.2254	0.1217

+Experimental data are from Yucelen and Kidnay [63].

Table 11. Results for multicomponent mixtures

T, K	Component	X(ex)	Y(ex)	Y(VDW)	Y(MWS)
322	N_2	0.00051	0.002610	0.002950	0.002366
	CO_2	0.19275	0.284870	0.251429	0.256226
	C_1	0.25660	0.659520	0.689775	0.692733
	C_2	0.02253	0.020050	0.021821	0.020416
	C_3	0.03103	0.014200	0.015205	0.013030
	C_4	0.04853	0.010290	0.010478	0.009503
	C_5	0.03392	0.003710	0.003596	0.002792
	C_6	0.02618	0.001430	0.001494	0.001069
	C_7	0.04456	0.001250	0.001359	0.000826
	C_8	0.04578	0.000678	0.000712	0.000437
	C_{10}	0.25967	0.001370	0.001164	0.000597
	C_{14}	0.03794	0.000026	0.000017	0.000006
	P (ex), bar P (cal), bar			103.7 98.8	103.7 101.4
339	CO_2	0.68158	0.88304	0.878025	0.877137
	C_1	0.04082	0.08450	0.087702	0.090926
	C_2	0.00495	0.00519	0.005298	0.005926
	C_3	0.01106	0.00620	0.007482	0.008096
	C_4	0.01785	0.00703	0.007000	0.007615
	C_5	0.01432	0.00362	0.003546	0.003764
	C_6	0.01235	0.00195	0.001960	0.001881
	C_7	0.02168	0.00226	0.002371	0.001909
	C_8	0.02305	0.00154	0.001633	0.001399
	C_{10}	0.15023	0.00450	0.004831	0.001269
	C_{14}	0.02211	0.00017	0.000153	0.000078
	P (ex), bar P (cal), bar			103.7 101.5	103.7 104.4

+Experimental data are from Turek et al., [2].

Table 12. Dew point pressure calculations for fluid OO-L-544

Temperature (K)	$P_{experimental}$ (bar)	$P_{calculated}$ (bar)
300	395.0	389.0
350	375.0	371.0
400	330.0	327.5

Table 13. Bubble point pressure comparisons for oil A.

	Oil A (Experiment)	Oil A (Calculated)	Oil E (Experiment)	Oil E (Calculated)	Oil F (Experiment)	Oil F (Calculated)
Temp. (^{o}C)	Pressure (psi)	Pressure (psi)	Pressure (psi)	Pressure (psi)	Pressure (psi)	Pressure (psi)
100	< 14.7	< 14.7	< 14.7	< 14.7	< 14.7	< 14.7
125	36	38.0	< 14.7	< 14.7	< 14.7	< 14.7
150	45	52.3	< 14.7	< 14.7	< 14.7	15.9
175	62	70.2	18.5	19.8	18.7	19.9

< 14.7 means pressure below atmospheric.

TABLE 14. Bubble point pressure comparisons for oils A, E and F.

	Oil A	Oil E	Oil F
Temperature (^{o}C)	Pressure (bar)	Pressure (bar)	Pressure (bar)
150	3.558	SP	1.028
175	4.776	1.347	1.352
200	6.268	1.821	1.760
225	9.956	2.426	2.265
250	12.085	3.185	2.883

SP = bubble pressure below 1 bar. All are calculated data.

Table 15. Vapor-liquid equilibrium data for oil A at different temperatures.

	T (K) =	398.3	423.3	448.3
Component	$X_{composition}$	$Y_{calculated}$	$Y_{calculated}$	$Y_{calculated}$
C_1	0.000510	0.1075	0.0800	0.0600
C_2	0.192750	0.1875	0.16040	0.1359
C_3	0.256600	0.1972	0.1811	0.1638
C_4	0.022530	0.1527	0.1531	0.1493
C_5	0.031030	0.1462	0.1588	0.1667
C_6	0.048530	0.0806	0.0979	0.1131
C_7^*	0.033920	0.1231	0.1581	0.1919
C_8^*	0.026180	0.0048	0.0098	0.0178
C_9^*	0.044560	0.0002	0.0006	0.0015
C_{10}^*	0.259670	0.0000	0.0000	0.0000
	P (bar) =	2.594	3.573	4.792

Table 16. Vapor-liquid equilibrium data for oil E at different temperatures.

	T (K) =	448.3	498.3	523.3
Component	$X_{composition}$	$Y_{calculated}$	$Y_{calculated}$	$Y_{calculated}$
C_1	0.0002	0.03320	0.01814	0.01337
C_2	0.0018	0.14871	0.09903	0.07935
C_3	0.0054	0.19566	0.14496	0.12185
C_4	0.0097	0.18764	0.15695	0.13905
C_5	0.0132	0.14297	0.13500	0.12580
C_6	0.0163	0.07339	0.08190	0.08219

C_7^*	0.1309	0.15641	0.22907	0.25784
C_8^*	0.2881	0.05814	0.12204	0.16003
C_9^*	0.1592	0.00388	0.01289	0.02046
C_{10}^*	0.3752	0.00000	0.00002	0.00007
	P (bar) =	1.347	2.426	3.185

Table 17. Vapor-liquid equilibrium data for oil F at different temperatures.

	T (K) =	448.3	498.3	523.3
Component	$X_{composition}$	$Y_{calculated}$	$Y_{calculated}$	$Y_{calculated}$
C_1	0.0009	0.1281	0.0756	0.0577
C_2	0.0024	0.1793	0.1296	0.1078
C_3	0.0045	0.1400	0.1112	0.0972
C_4	0.0077	0.1619	0.1457	0.1334
C_5	0.0097	0.1383	0.1404	0.1350
C_6	0.0125	0.0642	0.0778	0.0809
C_7^*	0.1481	0.1765	0.2801	0.3260
C_8^*	0.3368	0.0105	0.0341	0.0536
C_9^*	0.0893	0.0013	0.0050	0.0084
C_{10}^*	0.3881	0.0000	0.0000	0.0001
	P (bar) =	1.352	2.265	2.883

Table 18. Vapor-liquid equilibrium data for oil B at different temperatures.

	T (K) =	398.3	423.3	448.3
Component	$X_{composition}$	$Y_{calculated}$	$Y_{calculated}$	$Y_{calculated}$
H_2O	0.0590	0.0022	0.0040	0.0067
C_1	0.2694	0.8536	0.8063	0.7459
C_2	0.0142	0.0197	0.0213	0.0224
C_3	0.0286	0.0260	0.0298	0.0332
C_4	0.0416	0.0228	0.0282	0.0340
C_5	0.0714	0.0311	0.0395	0.0491
C_6	0.0902	0.0145	0.0216	0.0311
C_7^*	0.2587	0.0291	0.0466	0.0716
C_8^*	0.1020	0.0011	0.0026	0.0059
C_9^*	0.0123	0.0000	0.0000	0.0002
C_{10}^*	0.0528	0.0000	0.0000	0.0000
	P (bar) =	130.784	135.814	143.050

FIGURES

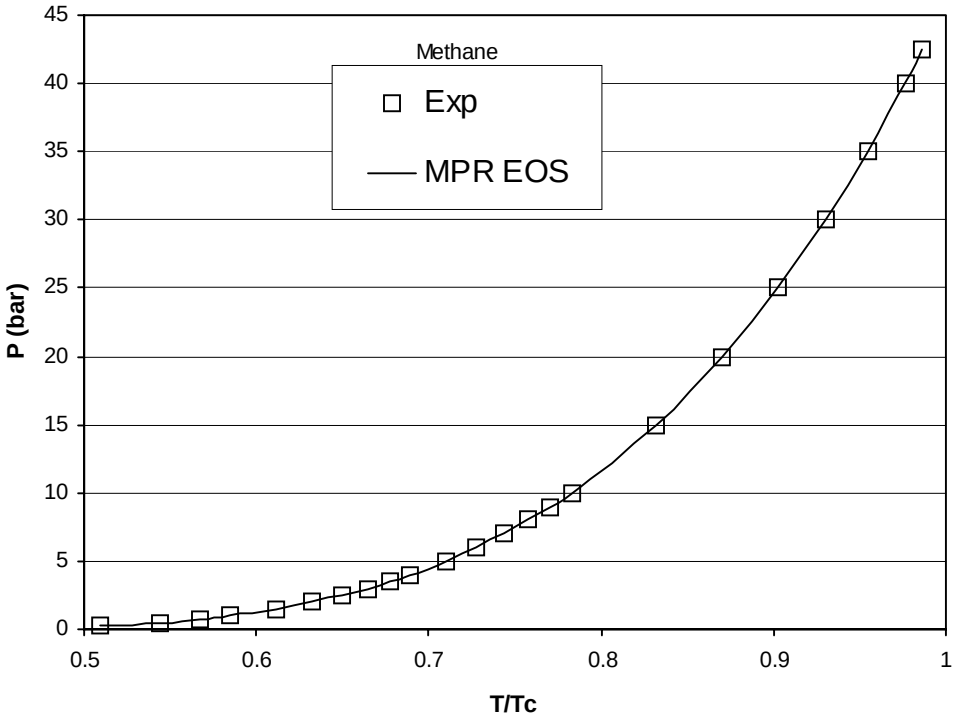

Fig. 1. Comparison of calculated results with experimental data of saturated vapor pressure of methane.

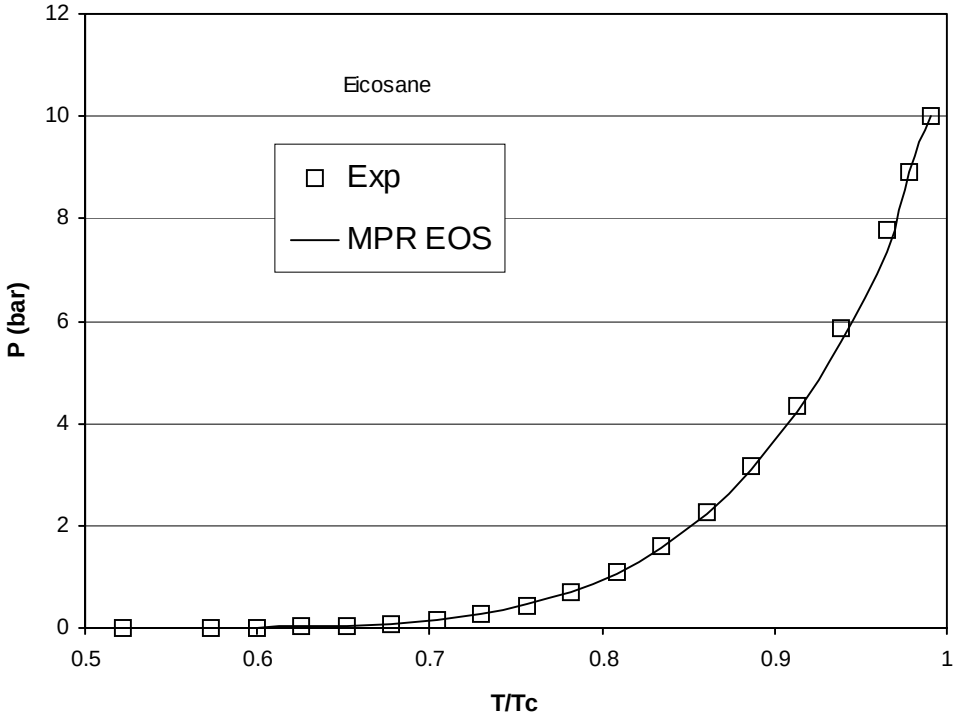

Fig. 2. Comparison of calculated results with experimental data of saturated vapor pressure of eicosane.

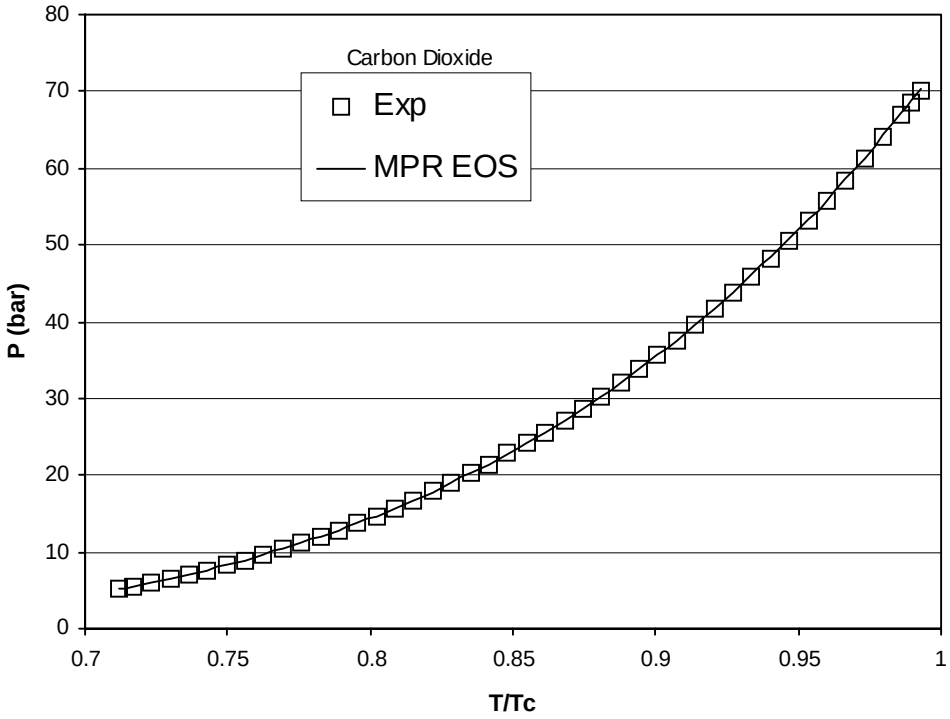

Fig. 3. Comparison of calculated results with experimental data of saturated vapor pressure of carbon dioxide.

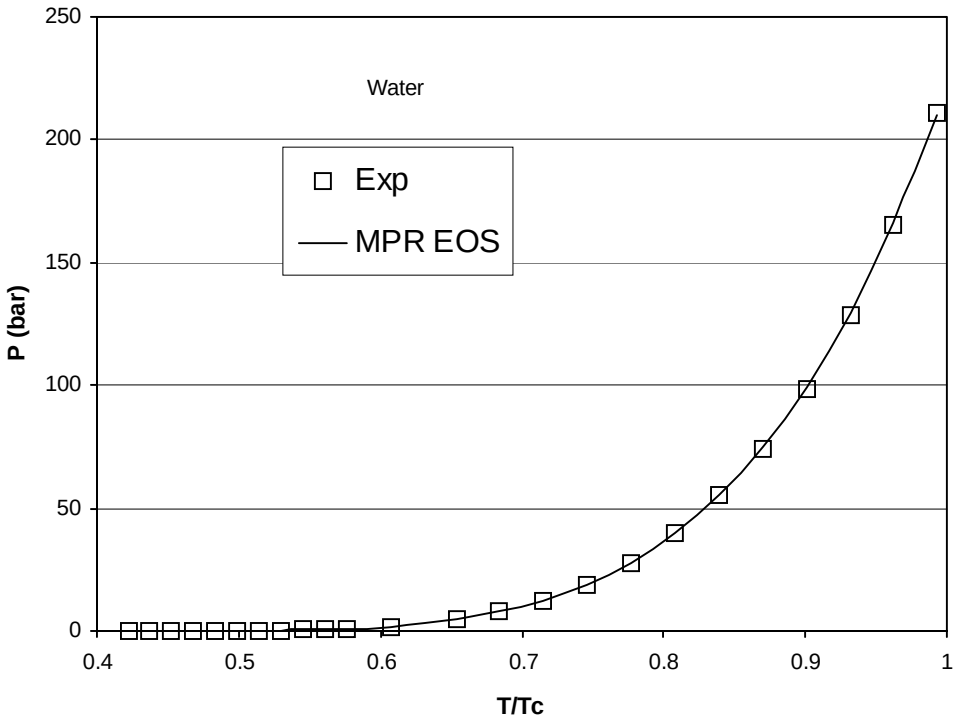

Fig. 4. Comparison of calculated results with experimental data of saturated vapor pressure of water

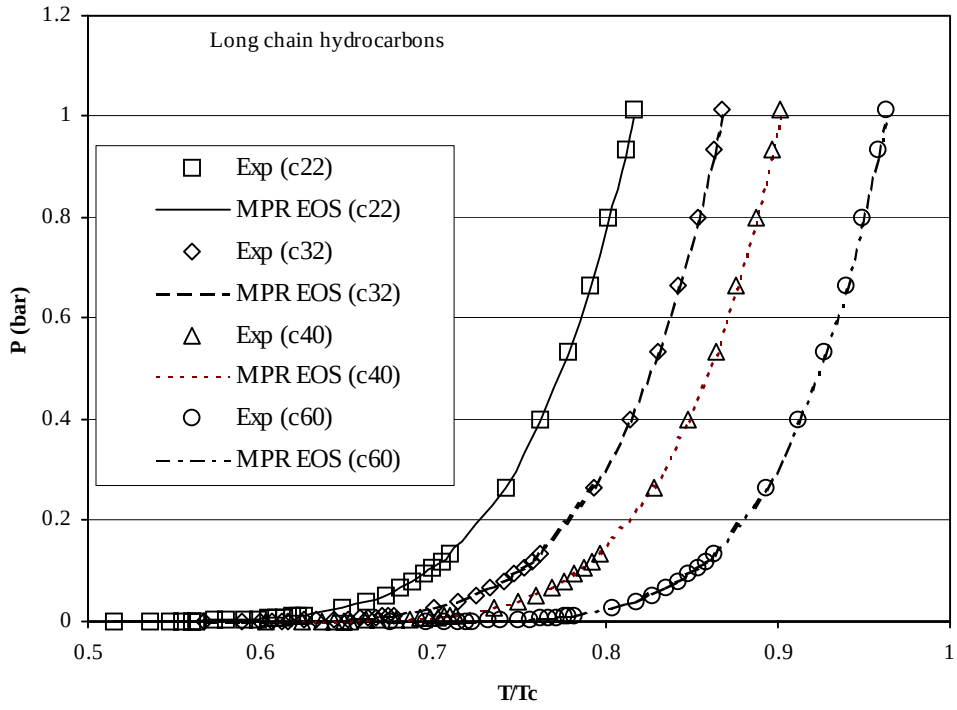

Fig. 5. Comparison of calculated results with experimental data of saturated vapor pressure of long chain hydrocarbons.

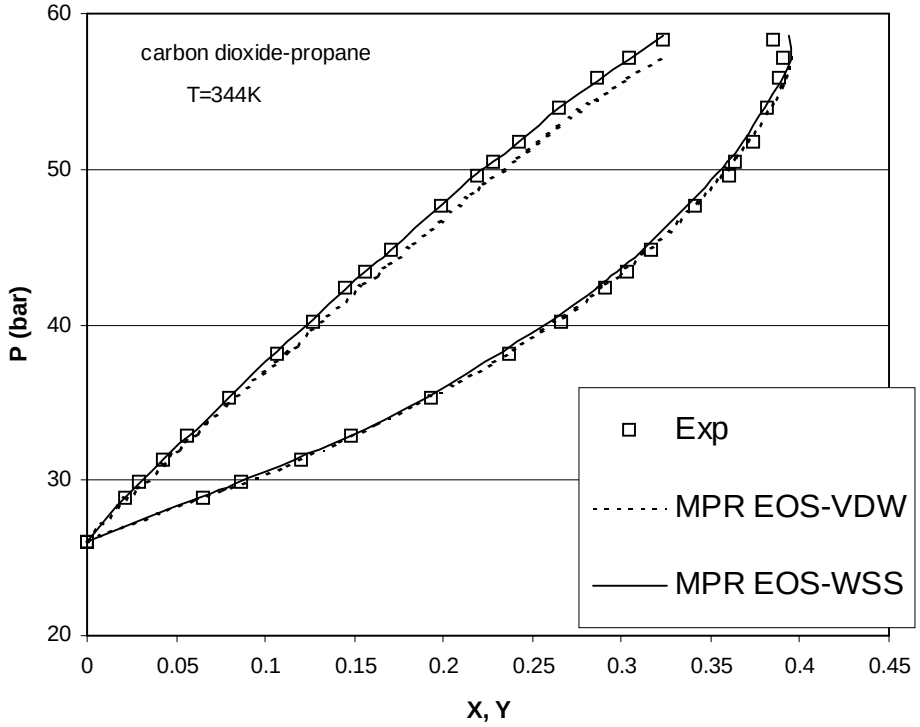

Fig. 6. Vapor/liquid equilibria of carbon dioxide/propane from MPR EOS/MWS MR and experiment (Reamer et al., 1951) at T=278K.

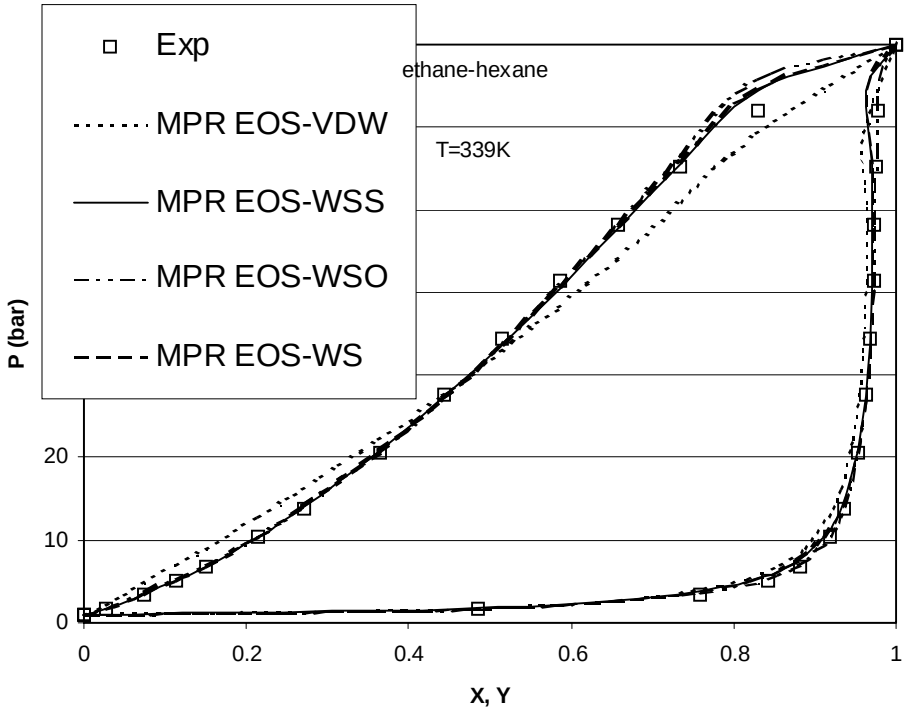

Fig. 7. Vapor/liquid equilibria of ethane/hexane from MPR EOS/MWS MR and experiment (Knapp et al.,1951) at T=339K.

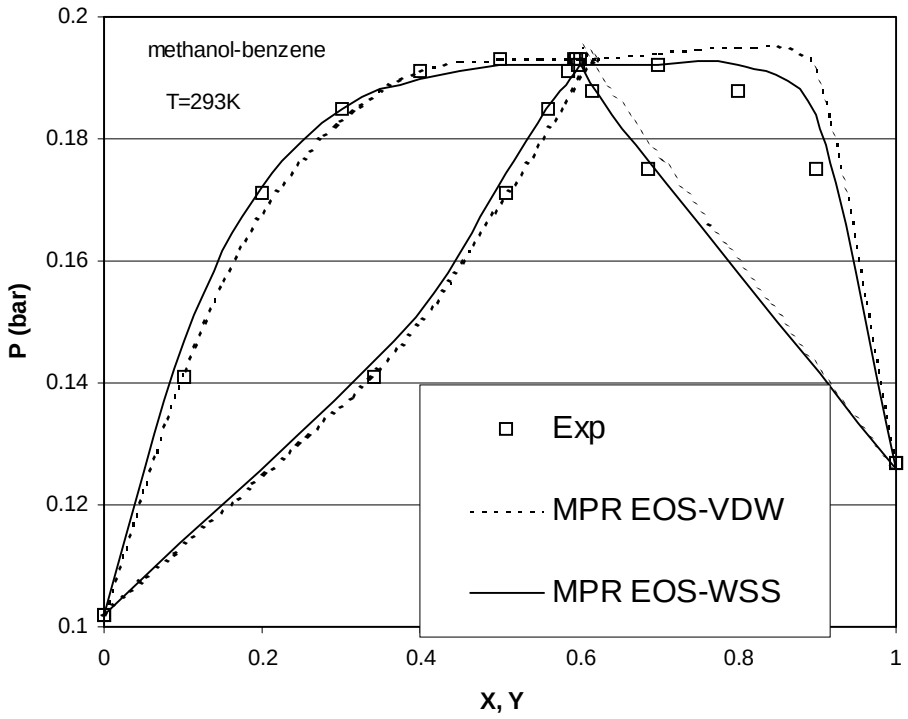

Fig. 8. Vapor/liquid equilibria of benzene/methanol from MPR EOS/MWS MR and experiment (Gmehling et al., 1982) at T=308K.

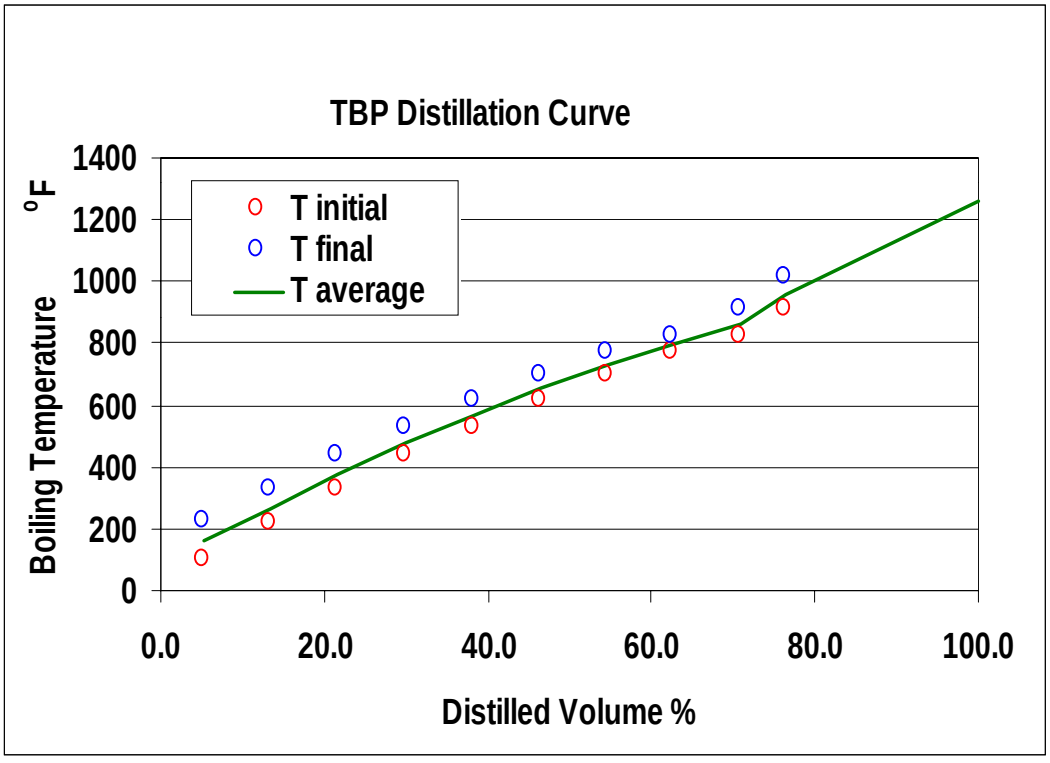

Fig. 9. True boiling point distillation curve for a standard oil.

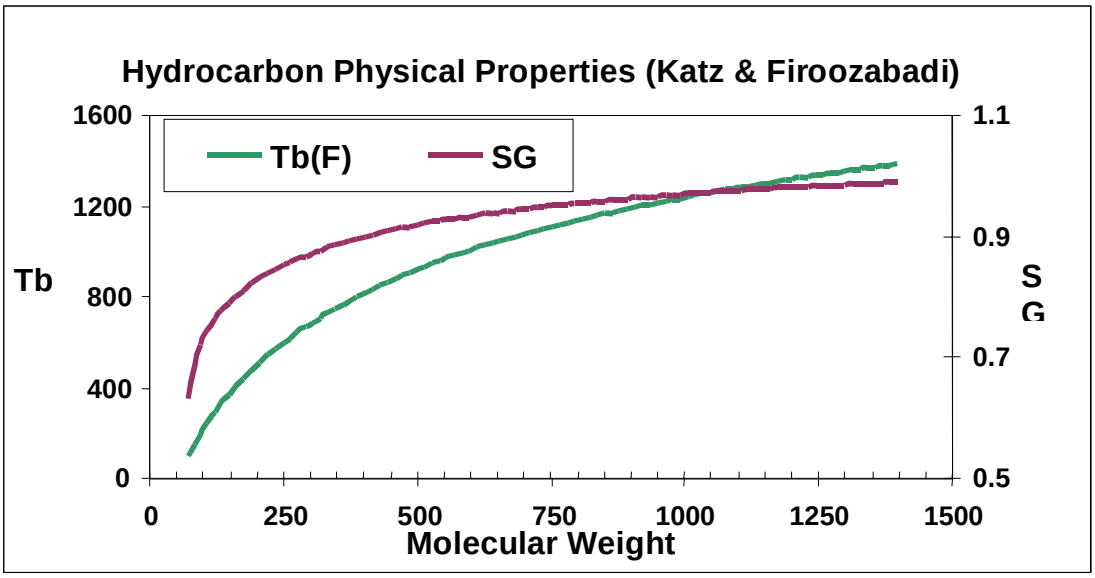

Fig. 10. True boiling point as a function of molecular weight for a standard oil.

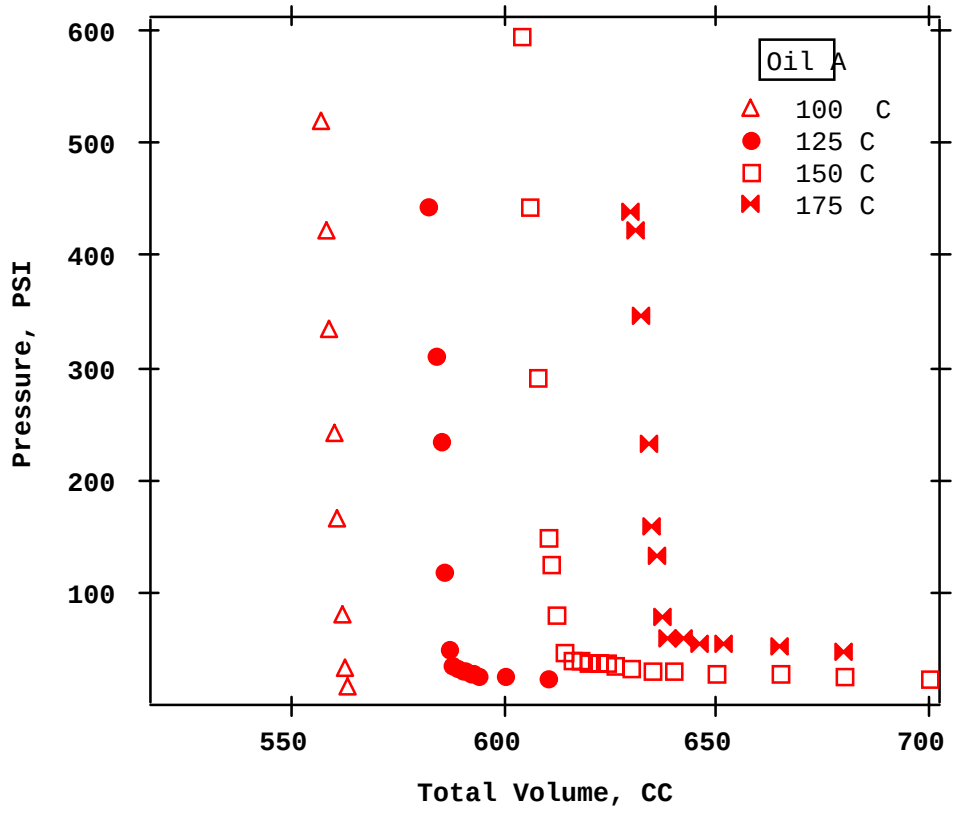

Fig. 11. Pressure Volume relation for Oil A at various temperatures.

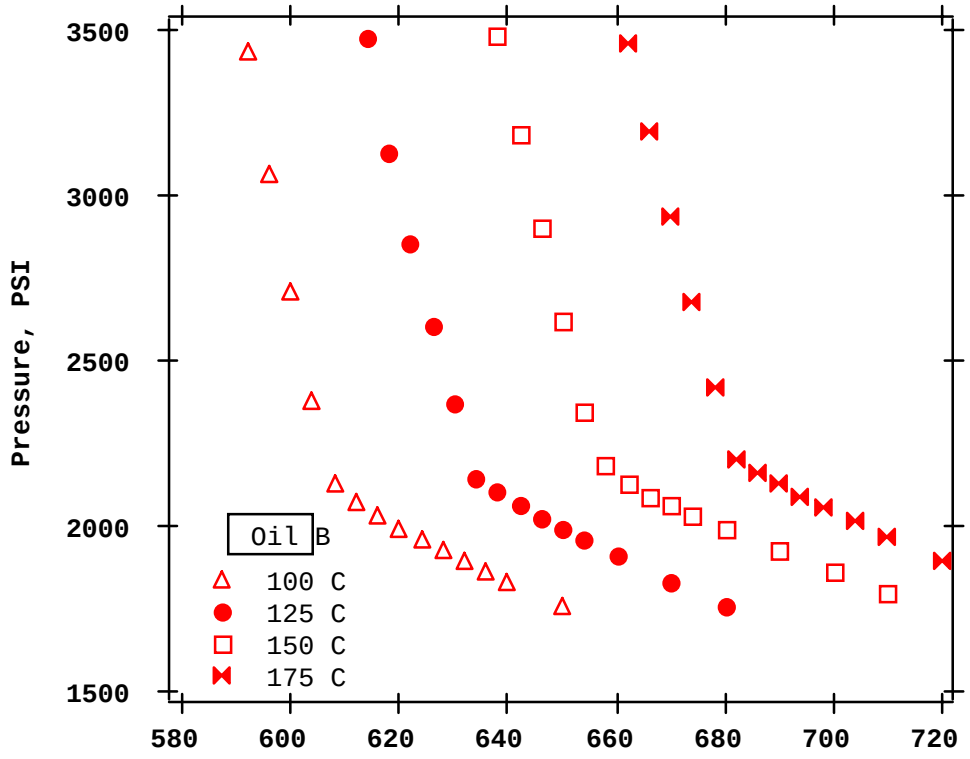

Fig. 12. Pressure Volume relation for Oil B at various temperatures.

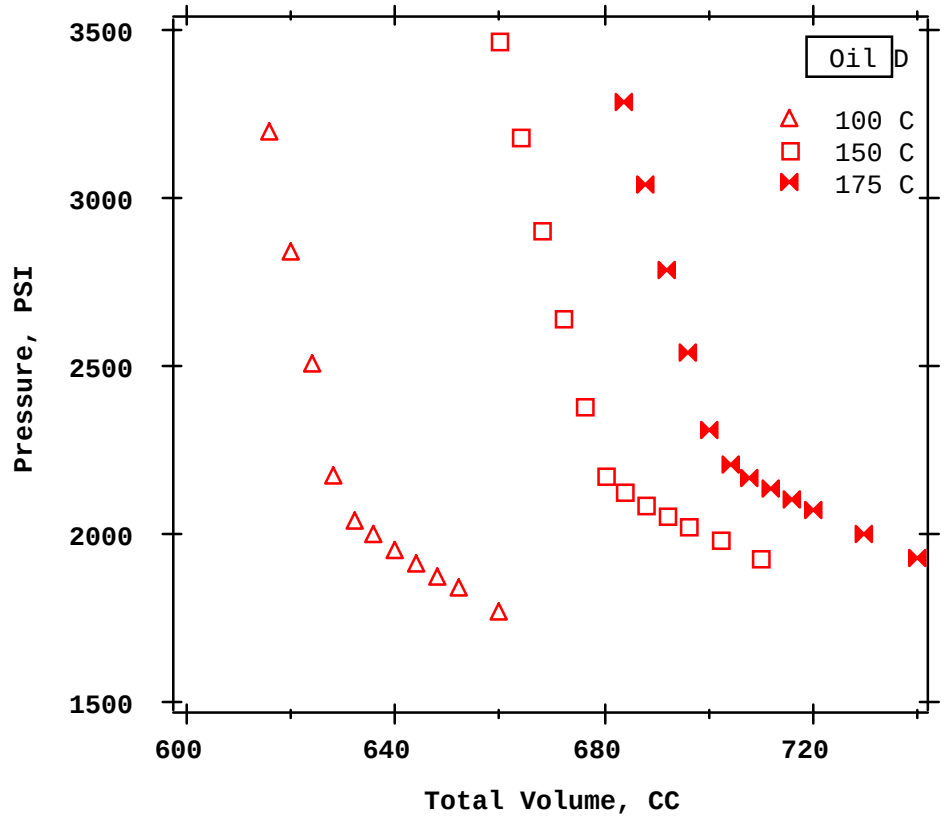

Fig. 13. Pressure Volume relation for Oil D at various temperatures.

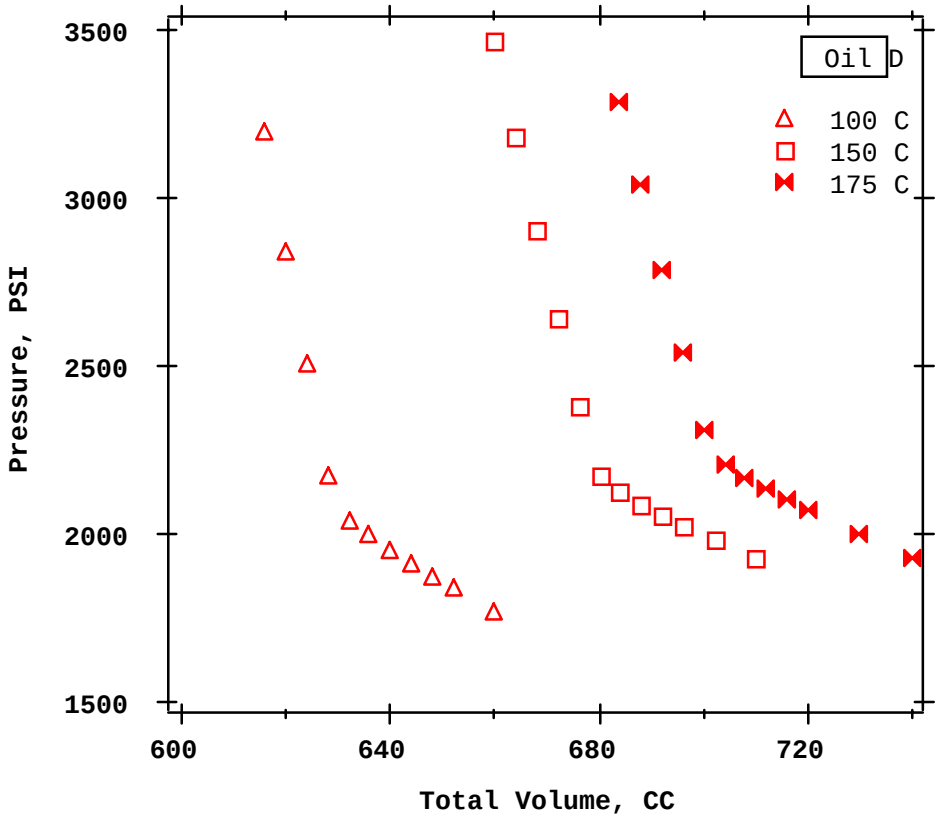

Fig 14. Pressure Volume relation for Oil D at various temperatures.

TRANSPORT AND PHASE EQUILIBRIA PROPERTIES FOR STEAM FLOODING OF HEAVY OILS

EDUCATIONAL ACTIVITIES

PUBLICATIONS

The paper "New Mixing Rules and Volume Correction Scheme for Phase Equilibria Calculations of Complex Hydrocarbon Mixtures." By K. Shukla and J. Gabitto has been submitted for publication to the Journal of Fluid Phase.

The paper "New Mixing Rules and Volume Correction Scheme for Calculations of Complex Hydrocarbon Mixtures Phase Equilibrium." By K. Shukla and J. Gabitto has been published in the Proceedings of the AIChE Annual Meeting, Los Angeles, November 2000.

The same paper was presented in the aforementioned meeting.

STUDENTS INVOLVED IN THE PROJECT

Mr. Oscar Eta, a Prairie View A&M University graduate student has worked on the project since January 2000. He completed in 2002 his Master Thesis, “Phase Equilibrium Calculations for Oil Mixtures.” under the advising of Dr. Gabitto.

Mr. Norman Alban has worked on this research project since March 2000. Mr. Alban completed his Master Thesis, “Surfactant-Polymer Interactions in Oil Recovery” in 2001 under the advising of Dr. Gabitto.

Mr. Joseph Etsibah, a Prairie View A&M undergraduate student, has also worked during Academic years, 2000/2001 and 2001/2002 on this project.

APPENDIX

The tables listed in the Appendix have been prepared in a such a way to maximize the amount of information in the minimum possible space. A brief explanation is provided here. The first three columns list the single carbon number fractions (SCN) along with the corresponding molar fractions and molecular weights obtained from the TBP tests. The first six rows also list the thermodynamic properties; T_b, T_c, P_c ,V_c and w, for the first six single carbon number fractions. The thermodynamic properties of the first four fractions are constant for all the oil samples and we found only small variations on the values of the fifth and sixth fractions, therefore, we used always the same values for the first six fractions for all the oils considered in this work. The rows from the seventh on present the thermodynamic properties corresponding to the pseudo-components calculated using Whitson's procedure [53]. A small independent table on the right bottom corner summarizes the information corresponding to the pseudo-components including, number, molar fractions, molecular weights and thermodynamic properties. The oil samples that are listed by number are data taken from Schou Pederssen et al. [51].

Table A1. Oil A Composition and Properties

Component	Molar Fractions	Molecular Weight	T_b (K)	T_c (K)	P_c (bar)	V_c (cm^3/mol)	ω
C_1	0.0047	16.0	111.7	190.6	45.4	98.0	0.008
C_2	0.0210	30.1	184.5	305.4	48.2	148.0	0.098
C_3	0.0423	43.5	231.1	369.8	41.9	203.0	0.152
C_4	0.0617	56.8	272.7	425.2	37.5	255.0	0.193
C_5	0.1058	71.1	309.2	469.6	33.3	304.0	0.231
C_6	0.1336	84.8	341.9	507.4	29.3	370.0	0.296
C_7^*	0.1135	88.1	372.0	540.5	26.9	427.8	0.353
C_8^*	0.0943	99.7	469.1	639.7	19.5	663.3	0.519
C_9^*	0.0785	112.6	557.2	717.3	14.0	975.7	0.709
C_{10}^*	0.0544	131.8	752.5	852.8	5.0	2796.7	1.430
C_{11}	0.0426	146.7					
C_{12}	0.0363	160.1					
C_{13}	0.0310	173.9					
C_{14}	0.0278	186.0					
C_{15}	0.0212	201.3	Number of Pseudo-components = 4				
C_{16}	0.0186	212.9	MW Limits		Comp. Range	Molar Fractions	Average MW

C_{17}	0.0162	230.4	88.10	130.02	7 - 9	0.3529	98.46
C_{18}	0.0118	244.6	130.02	191.88	10 - 14	0.2928	157.50
C_{19}	0.0064	252.6	191.88	283.17	15 - 19	0.1289	219.66
C_{20}	0.0783	417.9	283.17	417.90	20	0.1350	417.9

* Thermodynamic properties correspond to the pseudo-component fractions calculated on the right bottom of the table.

Table A2. Oil E Composition and Properties

Component	Molar Fractions	Molecular Weight	T_b (K)	T_c (K)	P_c (bar)	V_c (cm^3/mol)	ω
C_1	0.0002	16.0	111.7	190.6	45.4	98.0	0.008
C_2	0.0018	30.2	184.5	305.4	48.2	148.0	0.098
C_3	0.0054	44.1	231.1	369.8	41.9	203.0	0.152
C_4	0.0097	58.4	272.7	425.2	37.5	255.0	0.193
C_5	0.0132	72.5	309.2	469.6	33.3	304.0	0.231
C_6	0.0163	86.0	341.9	507.4	29.3	370.0	0.296
C_7^*	0.0198	90.6	417.7	589.1	23.2	528.9	0.426
C_8^*	0.0250	108.7	499.6	667.8	17.5	765.6	0.581
C_9^*	0.0295	122.6	572.7	730.2	13.1	1050.9	0.741
C_{10}^*	0.0566	135.8	764.0	858.8	4.7	2977.9	1.490
C_{11}	0.0572	148.7					
C_{12}	0.0549	161.8					
C_{13}	0.0640	175.4					
C_{14}	0.0581	191.1					
C_{15}	0.0539	203.5	Number of Pseudo-components = 4				
C_{16}	0.0487	214.8	MW Limits		Comp. Range	Molar Fractions	Average MW
C_{17}	0.0412	231.0	90.60	138.40	7 - 10	0.1309	124.70
C_{18}	0.0389	246.5	138.40	211.40	11 - 15	0.2881	177.40
C_{19}	0.0304	258.6	211.40	323.00	16 - 19	0.1592	238.44
C_{20}	0.3752	493.4	323.00	493.40	20	0.3752	494.30

* Thermodynamic properties correspond to the pseudo-component fractions calculated on the right bottom of the table.

Table A3. Oil F Composition and Properties

Component	Molar Fractions	Molecular Weight	T_b (K)	T_c (K)	P_c (bar)	V_c (cm^3/mol)	ω
C_1	0.0009	16.0	111.7	190.6	45.4	98.0	0.008

C_2	0.0024	30.3	184.5	305.4	48.2	148.0	0.098
C_3	0.0045	44.2	231.1	369.8	41.9	203.0	0.152
C_4	0.0077	58.3	272.7	425.2	37.5	255.0	0.193
C_5	0.0147	72.4	309.2	469.6	33.3	304.0	0.231
C_6	0.0175	86.5	341.9	507.4	29.3	370.0	0.296
C_7^*	0.0201	91.3	372.0	540.5	26.9	427.8	0.353
C_8^*	0.0283	110.4	499.6	667.8	17.5	765.6	0.581
C_9^*	0.0299	124.6	557.2	717.3	14.0	975.7	0.709
C_{10}^*	0.0456	134.7	752.5	852.8	5.0	2796.7	1.430
C_{11}	0.0472	148.8					
C_{12}	0.0539	162.3					
C_{13}	0.0644	176.3					
C_{14}	0.0691	189.4					
C_{15}	0.0589	204.1	Number of Pseudo-components = 4				
C_{16}	0.0418	217.2	MW Limits		Comp. Range	Molar Fractions	Average MW
C_{17}	0.0487	233.4	91.3	149.08	7 - 11	0.1711	129.82
C_{18}	0.0479	248.0	149.08	243.42	12 - 17	0.3368	230.21
C_{19}	0.0414	261.3	243.42	347.47	18 - 19	0.0893	254.17
C_{20}	0.3551	649.0	347.47	649.00	20	0.3551	649.00

* Thermodynamic properties correspond to the pseudo-component fractions calculated on the right bottom of the table.

Table A4. Oil G Composition and Properties

Component	Molar Fractions	Molecular Weight	T_b (K)	T_c (K)	P_c (bar)	V_c (cm^3/mol)	ω
H_2O	0.0590	18.0	111.7	190.6	45.4	98.0	0.008
C_1	0.2694	16.0	111.7	190.6	45.4	98.0	0.008
C_2	0.0142	30.1	184.5	305.4	48.2	148.0	0.098
C_3	0.0285	43.5	231.1	369.8	41.9	203.0	0.152
C_4	0.0416	56.8	272.7	425.2	37.5	255.0	0.193
C_5	0.0714	71.1	309.2	469.6	33.3	304.0	0.231
C_6	0.0902	84.8	341.9	507.4	29.3	370.0	0.296
C_7^*	0.0766	88.1	372.0	540.5	26.9	427.8	0.353
C_8^*	0.0636	99.7	469.1	639.7	19.5	663.3	0.519
C_9^*	0.0530	112.6	557.2	717.3	14.0	975.7	0.709
C_{10}^*	0.0367	131.8	752.5	852.8	5.0	2796.7	1.430
C_{11}	0.0287	146.7					
C_{12}	0.0245	160.1					
C_{13}	0.0209	173.9					
C_{14}	0.0188	186.0					

C_{15}	0.0143	201.3	Number of Pseudo-components = 4				
C_{16}	0.0126	212.9	MW Limits		Comp. Range	Molar Fractions	Average MW
C_{17}	0.0109	230.4	88.10	130.02	7 - 11	0.2587	108.67
C_{18}	0.0080	244.6	130.02	191.88	12 - 17	0.1020	148.54
C_{19}	0.0043	252.6	191.88	283.17	18 - 19	0.0123	219.66
C_{20}	0.0528	417.9	283.17	417.90	20	0.0528	417.9

* Thermodynamic properties correspond to the pseudo-component fractions calculated on the right bottom of the table.

Table A5. Oil 1 Composition and Properties

Component	Molar Fractions	Molecular Weight	T_b (K)	T_c (K)	P_c (bar)	V_c (cm^3/mol)	ω
C_1	0.0013	16.00	111.7	190.6	45.4	98.0	0.008
C_2	0.0050	30.10	184.5	305.4	48.2	148.0	0.098
C_3	0.0047	44.10	231.1	369.8	41.9	203.0	0.152
C_4	0.0117	58.10	272.7	425.2	37.5	255.0	0.193
C_5	0.0158	72.10	309.2	469.6	33.3	304.0	0.231
C_6	0.0189	86.20	341.9	507.4	29.3	370.0	0.296
C_7^*	0.0534	90.90	399.7	570.3000	24.58	487.130	0.396
C_8^*	0.0854	105.00	483.45	653.1300	18.52	705.720	0.548
C_9^*	0.0704	117.70	564.86	723.7000	13.56	1011.850	0.726
C_{10}^*	0.0680	132.00	662.69	806.0000	8.72	1398.140	1.022
C_{11}^*	0.0551	148.00	825.17	890.6100	3.20	3143.290	1.88
C_{12}	0.0500	159.00					
C_{13}	0.0558	172.00					
C_{14}	0.0508	185.00					
C_{15}	0.0380	197.00					
C_{16}	0.0267	209.00					
C_{17}	0.0249	227.00					
C_{18}	0.0214	243.00					
C_{19}	0.0223	254.00					
C_{20}	0.0171	262.00					
C_{21}	0.0142	281.00					
C_{22}	0.0163	293.00					
C_{23}	0.0150	307.00					
C_{24}	0.0125	320.00					
C_{25}	0.0145	333.00	Number of Pseudo-components = 5				
C_{26}	0.0133	346.00	MW Limits		Comp. Range	Molar Fractions	Average MW
C_{27}	0.0123	361.00	90.90	133.6300	7 - 10	0.2772	114.83
C_{28}	0.0115	374.00	133.63	196.43	11 - 14	0.2117	165.80

C_{29}	0.0109	381.00	196.43	288.76	15 - 21	0.1646	231.19
C_{30}	0.1828	624.00	288.76	424.48	22 - 29	0.1063	335.89
			424.49	624	30	0.1191	624.00

* Thermodynamic properties correspond to the pseudo-component fractions calculated on the right bottom of the table. Data from Schou Pedersen et al. [51].

Table A6. Oil 2 Composition and Properties

Component	Molar Fractions	Molecular Weight	T_b (K)	T_c (K)	P_c (bar)	V_c (cm^3/mol)	ω
C_1	0.0000	16.00	111.7	190.6	45.4	98.0	0.008
C_2	0.0001	30.1	184.5	305.4	48.2	148.0	0.098
C_3	0.0047	44.1	231.1	369.8	41.9	203.0	0.152
C_4	0.0209	58.1	272.7	425.2	37.5	255.0	0.193
C_5	0.1876	72.1	309.2	469.6	33.3	304.0	0.231
C_6	0.0437	86.2	341.9	507.4	29.3	370.0	0.296
C_7^*	0.0900	92.3	391.41	561.5100	25.3	468.780	0.383
C_8^*	0.1071	105.9	487.25	656.6200	18.3	717.360	0.555
C_9^*	0.0732	120.3	576.75	733.5700	12.9	1072.430	0.749
C_{10}^*	0.0623	133.0	720.82	810.1700	7.9	1407.900	1.026
C_{11}^*	0.0550	148.0	820.08	887.9600	3.3	3037.110	1.844
C_{12}	0.0514	163.0					
C_{13}	0.0443	177.0					
C_{14}	0.0480	190.0					
C_{15}	0.0381	204.0					
C_{16}	0.0282	217.0					
C_{17}	0.0333	235.0					
C_{18}	0.0234	248.0					
C_{19}	0.0266	260.0					
C_{20}	0.0418	269.0					
C_{21}	0.0171	283.0					
C_{22}	0.0148	298.0					
C_{23}	0.0156	310.0					
C_{24}	0.0113	322.0					
C_{25}	0.0112	332.0	Number of Pseudo-components = 5				
C_{26}	0.0097	351.0	MW Limits		Comp. Range	Molar Fractions	Average MW
C_{27}	0.0110	371.0	92.30	134.74	7 - 10	0.3326	110.46
C_{28}	0.0073	382.0	134.74	196.71	11 - 14	0.1987	168.49
C_{29}	0.0088	394.0	196.71	287.17	15 - 21	0.2085	242.30
C_{30}	0.0811	612.0	287.17	419.22	22 - 29	0.0897	338.29
			419.22	612.00	30	0.0811	612.00

* Thermodynamic properties correspond to the pseudo-component fractions calculated on the right bottom of the table. Data from Schou Pedersen et al. [51].

Table A7. Oil 4 Composition and Properties

Component	Molar Fractions	Molecular Weight	T_b (K)	T_c (K)	P_c (bar)	V_c (cm^3/mol)	ω
C_1	0.0003	16.0	111.7	190.6	45.4	98.0	0.008
C_2	0.0013	30.1	184.5	305.4	48.2	148.0	0.098
C_3	0.0036	44.1	231.1	369.8	41.9	203.0	0.152
C_4	0.0074	58.1	272.7	425.2	37.5	255.0	0.193
C_5	0.0152	72.1	309.2	469.6	33.3	304.0	0.231
C_6	0.0266	86.2	341.9	507.4	29.3	370.0	0.296
C_7^*	0.0925	89.8	387.56	557.38	25.57	460.42	0.378
C_8^*	0.1714	101.4	445.95	617.42	21.07	599.72	0.475
C_9^*	0.1190	116.1	570.84	728.66	13.22	1041.54	0.738
C_{10}^*	0.0800	134.0	756.00	854.78	4.89	2788.09	1.449
C_{11}	0.0605	148.0					
C_{12}	0.0526	161.0					
C_{13}	0.0570	175.0					
C_{14}	0.0427	189.0					
C_{15}	0.0379	203.0	Number of Pseudo-components = 4				
C_{16}	0.0286	216.0	MW Limits		Comp. Range	Molar Fractions	Average MW
C_{17}	0.0282	233.0	89.80	136.54	7 – 10	0.4630	108.47
C_{18}	0.0198	248.0	136.54	207.62	11 - 15	0.2510	141.31
C_{19}	0.0204	260.0	207.62	315.68	16 - 19	0.0970	236.73
C_{20}	0.1350	480.0	315.68	480.00	20	0.1350	480.00

* Thermodynamic properties correspond to the pseudo-component fractions calculated on the right bottom of the table. Data from Schou Pedersen et al. [51].

Table A8. Oil 5 Composition and Properties

Component	Molar Fractions	Molecular Weight	T_b (K)	T_c (K)	P_c (bar)	V_c (cm^3/mol)	ω
C_1	0.0005	16.0	111.7	190.6	45.4	98.0	0.008
C_2	0.0037	30.1	184.5	305.4	48.2	148.0	0.098
C_3	0.0117	44.1	231.1	369.8	41.9	203.0	0.152
C_4	0.0193	58.1	272.7	425.2	37.5	255.0	0.193
C_5	0.0236	72.1	309.2	469.6	33.3	304.0	0.231
C_6	0.0247	86.2	341.9	507.4	29.3	370.0	0.296
C_7^*	0.0652	88.8	372.82	541.4	26.83	429.42	0.354
C_8^*	0.0858	101.8	470.97	641.5	19.34	668.76	0.523
C_9^*	0.0486	116.1	556.61	716.85	14.04	973.24	0.708
C_{10}^*	0.0280	133.0	723.18	837.51	6	1783.69	1.278

C_{11}	0.0298	143.0					
C_{12}	0.0308	154.0					
C_{13}	0.0364	167.0					
C_{14}	0.0363	181.0					
C_{15}	0.0359	195.0	Number of Pseudo-components = 4				
C_{16}	0.0304	207.0	MW Limits		Comp. Range	Molar Fractions	Average MW
C_{17}	0.0360	225.0	88.80	131.19	7 – 9	0.1996	101.0356
C_{18}	0.0325	242.0	131.19	193.81	10 - 14	0.1613	157.3323
C_{19}	0.0307	253.0	193.81	286.32	15 - 19	0.1655	223.7184
C_{20}	0.3881	423.0	286.32	423.00	20	0.3881	423.0000

* Thermodynamic properties correspond to the pseudo-component fractions calculated on the right bottom of the table. Data from Schou Pedersen et al. [51].

Table A9. Oil 6 Composition and Properties

Component	Molar Fractions	Molecular Weight	T_b (K)	T_c (K)	P_c (bar)	V_c (cm^3/mol)	ω
C_1	0.0002	16.0	111.7	190.6	45.4	98.0	0.008
C_2	0.0020	30.1	184.5	305.4	48.2	148.0	0.098
C_3	0.0085	44.1	231.1	369.8	41.9	203.0	0.152
C_4	0.0160	58.1	272.7	425.2	37.5	255.0	0.193
C_5	0.0211	72.1	309.2	469.6	33.3	304.0	0.231
C_6	0.0239	86.2	341.9	507.4	29.3	370.0	0.296
C_7^*	0.0641	88.8	374.13	542.84	26.72	432.13	0.356
C_8^*	0.0884	101.8	470.45	641	19.38	667.24	0.522
C_9^*	0.0566	116.1	558.76	718.64	13.92	983.07	0.713
C_{10}^*	0.0376	133.0	716.27	833.91	6.26	1730.53	1.245
C_{11}	0.0365	143.0					
C_{12}	0.0366	154.0					
C_{13}	0.0465	167.0					
C_{14}	0.0439	181.0					
C_{15}	0.0451	195.0	Number of Pseudo-components = 4				
C_{16}	0.0386	209.0	MW Limits		Comp. Range	Molar Fractions	Average MW
C_{17}	0.0424	229.0	88.80	130.33	7 – 9	0.2091	101.69
C_{18}	0.0383	245.0	130.33	191.27	10 - 14	0.2011	156.98
C_{19}	0.0353	258.0	191.27	280.72	15 - 19	0.1997	225.65
C_{20}	0.3181	412.0	280.72	412.00	20	0.3181	412.00

* Thermodynamic properties correspond to the pseudo-component fractions calculated on the right bottom of the table. Data from Schou Pedersen et al. [51].

Table A10. Oil 6 Composition and Properties

Component	Molar Fractions	Molecular Weight	T_b (K)	T_c (K)	P_c (bar)	V_c (cm^3/mol)	ω
C_1	0.0000	16.0	111.7	190.6	45.4	98.0	0.008
C_2	0.0011	30.1	184.5	305.4	48.2	148.0	0.098
C_3	0.0121	44.1	231.1	369.8	41.9	203.0	0.152
C_4	0.0474	58.1	272.7	425.2	37.5	255.0	0.193
C_5	0.0524	72.1	309.2	469.6	33.3	304.0	0.231
C_6	0.0549	86.2	341.9	507.4	29.3	370.0	0.296
C_7^*	0.0983	92.8	391.35	561.44	25.26	468.64	0.383
C_8^*	0.1065	106.3	499.5	667.73	17.49	756.16	0.581
C_9^*	0.0710	120.9	580.54	736.72	12.67	1093.2	0.756
C_{10}^*	0.0606	134.0	789.18	871.87	4.06	2500.5	1.654
C_{11}	0.0508	148.0					
C_{12}	0.0420	161.0					
C_{13}	0.0447	175.0					
C_{14}	0.0341	189.0					
C_{15}	0.0325	203.0	Number of Pseudo-components = 4				
C_{16}	0.0270	216.0	MW Limits		Comp. Range	Molar Fractions	Average MW
C_{17}	0.0283	233.0	92.80	144.40	7 – 10	0.3364	110.43
C_{18}	0.0204	248.0	144.40	224.68	11 - 16	0.2311	177.31
C_{19}	0.0230	260.0	224.68	349.61	17 - 19	0.0717	245.93
C_{20}	0.1988	544.0	349.61	544.00	20	0.1988	544.00

* Thermodynamic properties correspond to the pseudo-component fractions calculated on the right bottom of the table. Data from Schou Pedersen et al. [51].

Table A11. Oil 9 Composition and Properties

Component	Molar Fractions	Molecular Weight	T_b (K)	T_c (K)	P_c (bar)	V_c (cm^3/mol)	ω
C_1	0.0000	16.0	111.7	190.6	45.4	98.0	0.008
C_2	0.0017	30.1	184.5	305.4	48.2	148.0	0.098
C_3	0.0129	44.1	231.1	369.8	41.9	203.0	0.152
C_4	0.0246	58.1	272.7	425.2	37.5	255.0	0.193
C_5	0.0283	72.1	309.2	469.6	33.3	304.0	0.231
C_6	0.0281	86.2	341.9	507.4	29.3	370.0	0.296
C_7^*	0.0621	90.5	387.21	557	25.6	459.64	0.376
C_8^*	0.0716	104.2	487.39	656.75	18.26	7117.79	0.556
C_9^*	0.0505	119.2	563.73	722.77	13.63	1006.43	0.723
C_{10}^*	0.0329	134.0	738.24	845.35	5.47	1910.84	1.353
C_{11}	0.0467	149.0					

C_{12}	0.0345	164.0					
C_{13}	0.0434	176.0					
C_{14}	0.0387	188.0					
C_{15}	0.0449	203.0	Number of Pseudo-components = 4				
C_{16}	0.0281	214.0	MW Limits		Comp. Range	Molar Fractions	Average MW
C_{17}	0.0360	232.0	92.50	134.84	7 – 10	0.2171	108.29
C_{18}	0.0308	248.0	134.80	200.91	11 – 14	0.1633	168.59
C_{19}	0.0367	259.0	200.91	299.34	15 - 19	0.1765	230.16
C_{20}	0.3436	446.0	299.34	446.00	20	0.3436	448.00

* Thermodynamic properties correspond to the pseudo-component fractions calculated on the right bottom of the table. Data from Schou Pedersen et al. [51].

Table A12. Oil 11 Composition and Properties

Component	Molar Fractions	Molecular Weight	T_b (K)	T_c (K)	P_c (bar)	V_c (cm^3/mol)	ω
C_1	0.0000	16.0	111.7	190.6	45.4	98.0	0.008
C_2	0.0010	30.1	184.5	305.4	48.2	148.0	0.098
C_3	0.0012	44.1	231.1	369.8	41.9	203.0	0.152
C_4	0.0021	58.1	272.7	425.2	37.5	255.0	0.193
C_5	0.0021	72.1	309.2	469.6	33.3	304.0	0.231
C_6	0.0045	86.2	341.9	507.4	29.3	370.0	0.296
C_7^*	0.0121	90.8	406.93	577.89	24	503.59	0.408
C_8^*	0.0187	106.5	498.88	667.17	17.53	754.12	0.58
C_9^*	0.0195	122.0	571.68	729.36	13.17	1045.85	0.739
C_{10}^*	0.0556	135.0	752.50	852.80	5.01	2047.81	1.427
C_{11}	0.0472	149.0					
C_{12}	0.0549	162.0					
C_{13}	0.0640	176.0					
C_{14}	0.0681	189.0					
C_{15}	0.0539	202.0	Number of Pseudo-components = 4				
C_{16}	0.0358	213.0	MW Limits		Comp. Range	Molar Fractions	Average MW
C_{17}	0.0487	230.0	90.50	137.18	7 – 10	0.1259	118.73
C_{18}	0.0489	244.0	137.18	207.24	11 – 15	0.2881	176.85
C_{19}	0.0404	256.0	207.24	313.10	16 - 19	0.1538	237.52
C_{20}	0.3976	473.0	313.10	473.00	20	0.3976	473

* Thermodynamic properties correspond to the pseudo-component fractions calculated on the right bottom of the table. Data from Schou Pedersen et al. [51].

Table A13. Oil 14 Composition and Properties

Component	Molar Fractions	Molecular Weight	T_b (K)	T_c (K)	P_c (bar)	V_c (cm^3/mol)	ω
C_1	0.0000	16.0	111.7	190.6	45.4	98.0	0.008
C_2	0.0004	30.1	184.5	305.4	48.2	148.0	0.098
C_3	0.0041	44.1	231.1	369.8	41.9	203.0	0.152
C_4	0.0135	58.1	272.7	425.2	37.5	255.0	0.193
C_5	0.0247	72.1	309.2	469.6	33.3	304.0	0.231
C_6	0.0322	86.2	341.9	507.4	29.3	370.0	0.296
C_7*	0.0763	91.0	389.59	559.56	25.4	464.82	0.38
C_8*	0.1010	104.1	485.91	655.39	18.36	713.23	0.553
C_9*	0.0678	118.5	563.57	722.63	13.64	1005.65	0.723
C_{10}*	0.0552	134.0	736.50	844.40	5.53	1895.09	1.344
C_{11}	0.0460	148.0					
C_{12}	0.0411	161.0					
C_{13}	0.0444	176.0					
C_{14}	0.0370	189.0					
C_{15}	0.0354	203.0	Number of Pseudo-components = 4				
C_{16}	0.0297	216.0	MW Limits		Comp. Range	Molar Fractions	Average MW
C_{17}	0.0309	233.0	92.50	135.33	7 – 10	0.3003	109.52
C_{18}	0.0250	248.0	135.33	201.23	11 – 14	0.1685	167.55
C_{19}	0.0277	260.0	201.23	299.25	15 - 19	0.1487	230.01
C_{20}	0.3034	445.0	299.25	445.00	20	0.3034	445.00

* Thermodynamic properties correspond to the pseudo-component fractions calculated on the right bottom of the table. Data from Schou Pedersen et al. [51].